I. POLYMER INDUCED ASSOCIATION AND KINETICS OF OXALOACETATE UTILIZING ENZYMES

II. PROTON AND MAGNESIUM BINDING TO 5-PHOSPHORIBOSYL α-1-PYROPHOSPHATE

By

TERESA ANN WEBSTER

Bachelor of Science

Eastern Washington State University

Cheney, Washington

1976

Submitted to the Faculty of the Graduate College
of the Oklahoma State University
in partial fulfillment of the requirements
for the Degree of
DOCTOR OF PHILOSOPHY
December, 1980

I. POLYMER INDUCED ASSOCIATION AND KINETICS OF OXALOACETATE UTILIZING ENZYMES

II. PROTON AND MAGNESIUM BINDING TO 5-PHOSPHORIBOSYL α-1-PYROPHOSPHATE

Thesis Approved:

H. Olin Spivey

Richard C Essenberg

Kent Carraway

K D Berlin

Franklin R. Leach

Norman N Durham

Dean of the Graduate College

ACKNOWLEDGMENTS

I would like to extend special thanks to my major adviser, Dr. H. Olin Spivey. Through his enthusiasm and guidance he has made these last four years a period of excitement and learning. In addition, gratitude is expressed to Dr. K. Darrell Berlin for his excellent help and advice with the NMR analyses. I also thank Dr. Richard Essenberg, Dr. Kermit Carraway, and Dr. Franklin Leach for their valuable time spent as members of the advisory committee.

Special appreciation is extended to Dr. Eric Manley who so patiently guided and advised me through my first stages of research. I wish to extend my gratitude for assistance received from Dr. Jerry Merz, Jim Appleman, John Hague, and Julie Arrington and also to express how much I enjoyed knowing and working with them. I extend my appreciation to Sue Heil, our departmental secretary, for her excellent job of typing this thesis.

And I especially thank my husband, Sam, for the love, encouragement, and sense of humor with which he supported me during these last four years. It is to Sam that I dedicate this thesis.

TABLE OF CONTENTS

Chapter Page

LIST OF TABLES

LIST OF FIGURES

LIST OF SYMBOLS AND ABBREVIATIONS

AAT or m-AAT	-	Mitochondrial aspartate amino transferase
c-AAT	-	Cytosolic aspartate aminotransferase
ADP	-	Adenosine 5'-diphosphate
AMP	-	Adenosine 5'-monophosphate
Asp	-	Aspartic acid
ATP	-	Adenine 5'-triphosphate
ATP-Sepharose	-	N^6-[6(Aminohexyl)Carbomoylmethyl]-ATP
BSA	-	Bovine serum albumin
CS	-	Citrate Synthase
D	-	Diffusion coefficient
DLS	-	Dynamic Light Scattering
DTP	-	Dimethyl 3,3'-dithiobispropionimidate
DTNB	-	5,5'-dithiobis(nitrobenzoic acid)
EDTA	-	Ethylenediaminetetraacetic acid
GDP	-	Guanosine 5'-diphosphate
Gln	-	Glutamine
Glu	-	Glutamic acid
GMP	-	Guanosine 5'-monophosphate
GTP	-	Guanosine 5'-triphosphate
K_m	-	Michaelis constant for a substrate
Mal	-	Malate
MDH or m-MDH	-	Mitochondrial malate dehydrogenase

c-MDH - Cytosolic malate dehydrogenase

Mr - Molecular weight

NAD^+ - β-Nicotinamide adenine dinucleotide

NADH - β-Nicotinamide adenine dinucleotide, reduced form

NMR - Nuclear magnetic resonance

OAA - Oxaloacetate

P-CoA - Palmitoyl-Coenzyme A

PEG - Polyethylene glycol

P - Monophosphate

PP - Pyrophosphate

PRPP - 5-phosphoribosyl α-1-pyrophosphate

$s_{20,w}$ - Sedimentation coefficient corrected to 20°C and water

TMS - Tetramethylsilane

V_{max} - Maximum velocity

Δ - Greek delta, indicating change

ε - Greek epsilon, indicating absorptivity

PART ONE

POLYMER INDUCED ASSOCIATION AND KINETICS OF OXALOACETATE UTILIZING ENZYMES

CHAPTER I

INTRODUCTION

As part of a general phenomenon of polymer interactions in solution, the presence of polymers in a solution of proteins may force certain proteins to associate. The effect of the polymer, polyethylene glycol on the self- and cross-association of the enzymes, mitochondrial malate dehydrogenase and citrate synthase, is reported in this thesis. Also reported is an investigation of possible anomalies in the kinetics of the coupled reactions catalyzed by malate dehydrogenase and aspartate aminotransferase.

Kinetics of the Coupled Reactions Catalyzed by AAT and MDH

The kinetic data of Bryce et al. (1) indicated anomalous behavior of the coupled aspartate aminotransferase and malate dehydrogenase reactions:

$$\text{aspartate} + \alpha\text{-ketoglutarate} \xrightarrow{\text{AAT}} \text{oxaloacetate} + \text{glutamate} \qquad (1\text{-}1a)$$

$$\text{oxaloacetate} + \text{NADH} \xrightarrow{\text{MDH}} \text{malate} + \text{NAD}^{+} \qquad (1\text{-}1b)$$

Usually when coupled enzymatic reactions are initiated (e.g. by adding aspartate to a mixture of the enzymes and other substrates in equations (1-1a) and (1-1b)), a lag phase is observed before the maximum rate of

the second reaction (NADH oxidation) is obtained. This is because a transient time, τ, is required for the concentration of the intermediate substrate, OAA, to build up to a steady-state level. The transient time can be predicted and is proportional to the K_m of the second enzyme under a broad range of conditions (1).

Bryce et al., however, observed no lag transient, although with their experimental resolution they should have detected one that was 1/8 that of the expected τ or longer. In effect MDH appeared to function with at least 8-fold lower OAA concentrations when using enzymatically generated OAA. Absence of the lag phase could result from association of the enzymes into an AAT-MDH complex. Thus, the intermediate could pass from the active site of the first enzyme to that of the next without dissociating from the enzyme complex. Using several methods, Bryce et al. found no evidence of such a complex.

Bryce et al. also observed "anomalous" kinetics using an independent method based on isotope ratios of reactant and product. [^{14}C]Aspartate was used as reactant and a pool of unlabeled OAA was added ("external" OAA) to the reaction mixture. If the enzymatically produced labeled OAA mixed with the pool of external unlabeled OAA, MDH could produce a pool of malate with a lower specific radioactivity than the aspartate. After quenching the reaction and isolating the malate by ion-exchange chromatography Bryce et al. found malate to have the same specific activity as the original substrate, aspartate. This implies that MDH reacted only with the enzymatically produced OAA and not with the external pool of OAA. The existence of an enzyme complex could possibly prevent the external OAA from binding; but, no such complexes were detected by the several methods used.

Therefore, Bryce et al. proposed that the aminotransferase produces an active oxaloacetate isomer, OAA_a, which reaches the dehydrogenase and is converted to malate before it can isomerize to its predominant form in aqueous solution. This OAA isomer model has broader implications than mentioned by Bryce et al., since the principle of microscopic reversibility requires that AAT exclusively uses the OAA isomer if the enzyme exclusively produces it. It would then be likely that all OAA utilizing enzymes use this enzymatically generated and active form of OAA with kinetic "anomalies" similar to those of AAT and MDH. Specifically, much lower K_m values would be expected for the enzyme mixture than with the separate enzymes in vitro. However, Manley et al. (2) observed no kinetic anomalies when they attempted to duplicate the lag-time experiments of Bryce et al.

In this thesis, I report isotope incorporation measurements like those of Bryce et al. which we made to clarify the discrepancies and questions raised. From these experiments we conclude that decomposition of OAA catalyzed by the ion-exchange resin make the results of Bryce et al. unreliable. Errors in their theoretical interpretations are also discussed.

Polymer Interactions in Solution

Polymer Induced Protein Associations

Recently, examples of polymer effects on protein associations have been documented. The presence of polymers in a protein solution often causes the related process protein precipitation and this effect can be

quite specific for the type of proteins affected. Most studies at this time report the effects of the polymer polyethylene glycol (PEG). However, the generality of these effects is indicated by several examples with dextran polymers and the related phenomenon of liquid-liquid separations (3). PEG is a crystalline, thermoplastic, water-soluble polymer with the general formula $H-(OCH_2CH_2)_n-OH$ (4) At high enough concentrations, it will precipitate most proteins, probably because of the combination of its good solubility in water with its hydrophobicity. At lower concentrations it will selectively precipitate certain proteins as described in the following reviews.

Homologous Associations. Ingham and Miekka (5) showed that PEG will selectively precipitate associated proteins while the same proteins, when unassociated or less associated, will remain soluble. For example, chymotrypsin and chymotrypsinogen self-associate at low ionic strength and raising ionic strength inhibits association. Comparison of the relative solubilities showed that 10-20% PEG precipitates the associated chymotrypsinogen and chymotrypsin in low ionic strength solutions. However, even 25% PEG cannot precipitate the less associated proteins in a high ionic strength solution. Another protein, β-lactoglobin, self-associates at pH 4.5 but not at pH 3 and 8. PEG could precipitate the β-lactoglobin at pH 4.5, but not at the pH extremes of 3 and 8. Glutamate dehydrogenase associates at neutral pH and was precipitated by 15% PEG. The combined presence of NADH and GTP (1 mM) prevented polymer formation and abolished precipitation. These results suggest in general that conditions that enhance self-association of proteins enhance their precipitability by PEG.

In the presence of certain microtubule associating proteins tubulin will self-associate into a characteristic microtubule structure. Herzog and Weber (6) found that PEG or dextran will induce tubulin to form normal microtubules in the absence of the microtubule associating proteins. The relative light scattering of tubulin in various concentrations of dextran and PEG was measured as a function of time (6). The light scattering initially increased rapidly in time then leveled to a plateau. Increasing polymer concentration increased the initial rate and final amount of associated or precipitated tubulin. It seemed a threshold amount of PEG (3%) was required to induce association, and the threshold was close to the PEG concentration (4.5%) at which visible precipitate appeared.

PEG and dextran also enhance the extent and rate of fibrin polymerization (clotting) (7). Rumpling and Lane also showed that the polymerizing effects of dextran on fibrin increase with the increasing molecular weight of dextran (8). Clotting requires the thrombin catalyzed conversion of fibrinogen to fibrin, which polymerizes to form large precipitates or clots. Several high molecular weight water soluble polymers: starch, polyvinyl alcohol, dextran, ficol, and PEG shorten the time for clot formation (7). That polymers have their effect on fibrin polymerization rather than on the activity of the thrombin was shown by Rumpling and Lane (8).

Heterologous Associations. Several studies indicate that in the presence of PEG heterologous complexes exist between the following five pairs of enzymes: m-AAT and m-MDH (9), MDH and GDH (10), CS and MDH (11), AAT and GDH (10), and c-AAT and c-MDH (9). It is noteworthy that

only these five pairs formed heterologous complexes, though their interaction with numerous other proteins were tested, and four of the five pairs are between enzymes adjacent to each other in their metabolic pathways. Fahien and Kmiotek (10) found that 14% PEG caused formation of the precipitated heterologous complexes between AAT and GDH and between MDH and GDH. This corresponded to the fact that in the absence of PEG a soluble heterologous complex can be detected between AAT and GDH (12). There is some evidence that a weak attraction may also exist between MDH and GDH in the absence of PEG (13). Palmitoyl-CoA binding greatly enhances the association between MDH and GDH and also the precipitability of the MDH-GDH pair by PEG (10). The precipitation of both pairs (AAT-GDH and MDH-GDH) by 14% PEG was quite specific in that all four enzymes when alone or mixed with several other protein types showed little precipitation.

In another study by Halper and Srere (11) 14% PEG was found to selectively precipitate the enzyme pair, MDH-CS. In this case the two enzymes do not complex in the absence of PEG. This precipitation is also specific in that each enzyme alone is soluble. MDH incubated alone or with nine other enzymes is soluble in 14% PEG. Also, CS incubated alone or with nine other enzymes (including c-MDH) is soluble in 14% PEG.

In all three cases; MDH-GDH, GDH-AAT, and MDH-CS, addition of the second enzyme does not cause insolubility of the mixture by simply raising the total protein concentration. The total enzyme concentration was too low for the presence of the second enzyme to affect the first. Also, substituting the second enzyme with other types of proteins does not cause precipitation. The only reasonable explanation is that each

pair formed a heterologous complex which was less soluble than either enzyme alone in PEG.

Association of a soluble mixture of AAT and MDH has been reported in the presence of the polymer mixture, dextran (50,000 MW) and trimethylaminopolyethyleneglycol (TMA-PEG), or carboxymethyl-polyethylene glycol (CM-PEG) (9). This test involved counter-current chromatography with aqueous biphasic systems made with these polymers. When MDH and AAT were chromatographed separately their peaks were well resolved. When these enzymes were chromatographed together these peak positions and shapes were greatly altered indicating significant interaction between the enzymes. This interaction was quite specific in that the cytoplasmic forms of the enzyme, c-AAT and c-MDH, interact with each other as do the mitochondrial forms, m-AAT and m-MDH; but, no interaction between a cytoplasmic enzyme and a mitochondrial one could be detected. It is possible that counter-current distribution chromatography was a sensitive enough method to detect a weak association between MDH and AAT that exists in the absence of polymers. However, this was the only method which detected interactions between these enzymes and several examples of polymer induced enzyme association are now known. Therefore, it seems more likely that the polymers in the biphasic system enhanced these interactions to an extent which might be detected by several methods.

Kinetics of Reversibly Associating Enzymes. The several studies described up to this point indicate that the presence of polymers can cause or enhance very specific interactions between proteins. The consequences of polymer induced enzyme associations on the kinetics

of these enzymes have not been studied, but kinetic studies of a few reversibly associating enzymes indicate that large catalytic changes can occur. For example, erythrocyte glucose-6-phosphate dehydrogenase associates in vitro at concentrations above 0.3 mg/ml to oligomers with about four times the specific activity of the protomers (14). When phosphofructokinase associates at cellular concentrations, its response to the modifiers fructose-6-phosphate and ATP are considerably altered (15, 16). Bovine liver glutamate dehydrogenase extensively associates at cellular enzyme concentrations and although its specific activity with saturating substrates does not change, binding of purine di- and tri-phosphates and kinetic inhibition by GDP is different with the oligomers compared with the enzyme protomers (17).

Several highly specific heterologous enzyme associations have been demonstrated and in nearly every instance they are limited to enzymes sharing a common substrate. GDH and AAT have been shown by several methods to form a heterologous complex. In this complex AAT delivers its pyridoxal cofactor as a substrate for the active site of GDH. GDH can then amidate and reduce the cofactor as shown in reaction (1-2a), instead of its normal substrate, α-KG. If OAA is also present, AAT will amidate it to form aspartate as in reaction (1-2b) (12).

$$\text{Pyridoxal phosphate-AAT}\bullet\text{GDH} + \text{NADH} + \text{NH}_4 \longrightarrow \text{Pyridoxamine-AAT}\bullet\text{GDH} + \text{NAD}^+ \qquad (1\text{-}2a)$$

$$\text{Pyridoxamine-AAT}\bullet\text{GDH} + \text{OAA} \longrightarrow \text{ASP} + \text{Pyridoxal phosphate-AAT}\bullet\text{GDH} \qquad (1\text{-}2b)$$

In the presence of palmitoyl-CoA MDH and GDH form a complex. In this complex MDH is completely protected from palmitoyl-CoA inhibition (13).

Phosphofructokinase and fructose bisphosphate phosphatase have been reported to associate causing several large changes in the properties of phosphofructokinase, including: 90% inhibition of its activity; approximately seven-fold decrease in K_i for ATP inhibition; approximately nine-fold decrease in the K_i of 3-P-glycerate inhibition, and approximately 3.5-fold increase in K_m of fructose-6-P (18).

Why should enzyme associations cause altered catalytic properties? A few reasons can be cited. Most generally, altered catalytic properties could result from the subunit conformational changes that are most often coupled to association equilibrium (19). It is also possible that enzyme association could partially or totally cover ligand binding sites. Another possible kinetic change can occur with heterologous associations if the enzymes share a common substrate. In this case "channeling" of the substrate directly between the complexed enzymes can occur rather than the first enzyme releasing the substrate into the media. This would greatly increase the effective concentration of the shared substrate and the efficiency of the overall process.

Polymer Induced Phase Separation

The ability of polymers to cause protein precipitation or association as described in this review is related to the ability they have to cause phase separation. This section describes the phase forming properties of polymers pertinent to this thesis and is based principally on an extensive review by Albertsson (3). More often than not when two different polymers are mixed phase separation will take place. Immiscible liquid layers will form, and one layer will contain predominantly one polymer and the other

will contain predominantly the second polymer. This phase separation can take place with low concentrations of polymers yielding phases which are greater than 98% water. For example, when a solution of dextran 1.1% in water is mixed with a solution of 0.36% methylcellulose in water, two phase will result. One phase will consist of 0.39% dextran 0.65% methylcellulose and 98.96% H_2O.

The ease of forming separate aqueous phases, as judged by the polymer concentrations needed, appears to be proportional to the differences in hydrophobicities between the two polymers. These differences, however, can be very small and even closely related, highly hydrophilic polymers will cause phase separation. For example, a high molecular weight dextran sulfate gives as many as 9 liquid phases when dissolved in 0.3 M NaCl at a total dextran sulfate concentration of 20% w/v. The phase separation in this case is most probably due to a combination of high molecular weight and the heterogeneity in the extent of sulfate substitution of the dextran molecules. The ease of phase separation (measured as the reciprocal of polymer concentration required) also increases at a greater than proportional rate with the increase of polymer molecular weight.

Either phase separation, polymer precipitation, or association can occur when two polymers are mixed. Each effect results from what Albertsson terms as "incompatibility" between the polymers which forces polymer 2 (P2) to increase its distance from polymer 1 (P1) and vice versa. P2 may increase its distance by moving into a separate phase or by self-association. The extent to which each occurs will depend on the relative interactions of P2 with itself and with the solvent. If P2-solvent attractions are greater than those of P2 with

itself, the free energy of the mixture may be reduced by forming separate solution phases. Then P2 may be enriched in one of the phases and the unfavorable interactions with P1 simultaneously reduced. On the other hand, if solvation of P2 is poor and made even poorer by the presence of P1, the mixed system may reach a lower free energy by precipitation of P2.

In the systems which I have previously discussed mixing of P1 (usually PEG) with P2 (the protein) resulted in precipitation of the protein. Phase separation rather than protein precipitation can occur. For example, in Albertsson's study (3), a mixture of BSA and PEG resulted in phase separation with one phase containing BSA and the second phase containing PEG. However, in the protein systems which are reviewed under "Homologous Associations" and "Heterologous Associations" the polymer is present in several thousand-fold molar excess to the protein. This relatively massive amount of polymer has a large repulsive effect on the protein while the small amount of protein has little effect on the polymer, so protein precipitation rather than phase separation occurs.

The specific molecular basis of the "incompatibility" between P1 and P2 is not at present known. It could in principle arise from direct P1-P2 repulsive forces, indirect repulsion mediated through polymer-solvent interactions, or excluded volume effects. However, polymer precipitation, association, or phase separation are related in that they are different ways in which "incompatible" polymers increase their distance between each other.

Properties of m-MDH and CS

Malate dehydrogenase was extensively reviewed by Banaszak and Bradshaw (20). It catalyzes the oxidation of L-malate by NAD^+ to form OAA plus NADH. The enzyme occurs in virtually all eukaryotic cells in at least two unique forms identified as mitochondrial MDH (m-MDH or often called "supernatant" MDH) according to their cellular location. The supernatant isozyme is generally considered to act on the cytoplasmic side of the "malate shuttle" providing a means of transporting NADH equivalants in the form of malate, across the mitochondrial membrane. The mitochondrial enzyme, in addition to its role in the other half of the malate shuttle, is also an essential component of the tricarboxylic acid cycle.

m-MDH Molecular Properties

Thorne et al. (21) extensively characterized the mitochondrial form of MDH from pig heart. The results, summarized in Table I, are as follows. Using the ratio of sedimentation velocity(s) to diffusion coefficient (D) they obtained a molecular weight (MW) of 70,000. The frictional ratio, f/f_o, calculated from these s and MW values is 1.4. Such a high frictional ratio might indicate a very asymmetric molecule with an axial ratio of approximately 8; however, this ignores any possible effects of hydration. The enzyme consists of two identical subunits with molecular weights of 35,000. Each enzyme molecule has been shown to bind two molecules of reduced coenzyme, one per subunit. The enzyme has no disulfide bridges, but has 14 sulfhydryl groups per 70,000 daltons. Optical rotation studies suggest that the helical content is between 35 and 40%. In the absence of disulfide bonds, the

TABLE I

MOLECULAR PROPERTIES OF MITOCHONDRIAL MDH

Property	Value
Molecular Weight	70,000
Number of Subunits	2
Molecular Weight/Subunit	35,000
Coenzyme Binding/Subunit	1
$s_{20,w}$	3.9 S
Diffusion Coefficient	5.2×10^{-7} cm_2/s
Fractional ratio f/f_o	1.4
Axial Ratio (assuming unhydrated molecule)	8
Extinction Coefficient, A_{280}	0.25 cm^{-1} ml/mg
Helical Content	35-40%
Disulfide Bridges	0
Sulfhydryl Groups	14
Fluorescence Max (Exc. at 280 nm)	305-310* nm

*This corresponds to the emission of tyrosine as m-MDH is devoid of tryptophan.

suggested asymmetry of the molecule might be expected to be maintained by a rigid tertiary structure. A proportion of helical coiling in the polypeptide chain would contribute to this requirement. m-MDH is a protein devoid of tryptophan. Therefore, its fluorescence, when excited at λ_{280}, results from tyrosine emission and has a maximum at 305 to 310 nm.

Nature of m-MDH Subforms

m-MDH has been shown to exist in multiple subforms by electrophoretic techniques (20). In the past the origin was attributed to conformational differences, combination of similar but nonidentical polypeptide chains, or proteolytic degradation. Recent studies have indicated that the probable origin in pig heart m-malate dehydrogenase is deamidation of asparaginyl and/or glutaminyl residues, thus the acidic subforms are probably preparation artifacts. Under appropriate conditions most of the enzyme can be recovered as subform A, the most basic band as judged electrophoretically.

Recently, Jones and Vestling (22) have considered possible sources of m-MDH isoelectric heterogenity other than artifactual changes introduced during the purification procedure. Their new, gentler isolation procedure for m-MDH from rat heart and liver was found to isolate several multiple forms. The multiple forms corresponded precisely to forms observed in fresh homogenates of either liver or heart and, therefore, could not be rationalized as artifacts of the purification procedure. The MDH from liver was separated into four forms isoelectric at pH 9.65, 9.4, 9.2, and 8.75. The heart enzyme had forms isoelectric at pH's 9.6, 9.4, and 8.9. There was no

significant difference between the amino acid compositions of the two sources. Subjecting enzyme from either sources to a freeze-thaw cycle with lysolecithin abolished multiplicity in both cases and converted both liver and heart enzyme to a single form isoelectric at pH 9.6. Subjecting either crude or purified m-MDH to phospholipase D generated acidic forms (pI of 5.2 to 5.6) like the supernatant MDH. Lipid analysis on extracts of the purified enzyme from both liver and heart demonstrated that variable but significant amounts of phospholipid and neutral lipid were bound to the purified enzyme from either source.

It has been postulated (22) that lipid binding may preserve the high level of amidation of Asp and Glu side chains. Removal of lipid during purification may result in extensively deamidated protein with pI around 6. The "gentle" procedure of Jones and Vestling does not extensively remove lipid and the MDH has isoelectric points between 8.75 and 9.6. Masking of ionic side-chains by variable amounts of tightly bound phospholipid may contribute to the existence of the multiple electrophoretic species with the hish isoelectric points.

Interaction of m-MDH with Lipids

Studies other than those of Jones and Vestling (21) (see "Nature of Subforms") describe MDH-lipid interactions and their possible consequence. Dodd (23) obtained NMR spectra of a mixture of lysolecithin and MDH finding that both the head group and hydrocarbon chains bind to the enzyme. MDH did not, however, bind lecithin. Since lysolecithin does not occur in natural membranes, the lysolecithin-enzyme interaction was not considered to be of direct physiological interest. However, the interaction may serve as a guide to a more

complex interaction between lecithin and enzyme. Webster et al. (24) found that native enzyme did not interact with phospholipid vesicles. In contrast an association of enzyme subunits with vesicles was demonstrated by several methods.

Some data indicate that lipids affect the properties of MDH in dilute solutions (20). Lysolecithin, but not lecithin, reduced the rate of thermal inactivation of MDH (20, 23, 25). Jones and Vestling (25) found that prior incubation of MDH with lysolecithin prevented a heat induced shift of the isoelectric point from 9 to 6.

Studies on the distribution of various enzymes inside the mitochondria indicate that m-MDH is one example of an intermediate class of mitochondrial enzymes (20). It may associate with the inner membrane matrix (20). Increasing levels of succinate and cations cause m-MDH to be released from the inner membrane. This association with both the matrix and inner membrane is not restricted to m-MDH since it is the property of other enzymes such as aspartate aminotransferase (20).

Catalytic Properties of m-MDH

When an enzyme contains multiple subunits and the reaction which it catalyzes involves multiple substrates, detailed steps in the catalytic process may become very complicated. The malate dehydrogenases contain two subunits, and the substrates include both a dicarboxylic acid and the dinucleotide coenzyme. The third reactant is a proton from the solvent. Data from both isotopic exchange rates and initial velocity studies are compatible with a compulsory ordered mechanism. In the case of pig heart m-MDH Harada and Wolfe (20) have

suggested that the compulsory ordered mechanism must be modified to account for the inhibitory effect of hydroxymalonate. The simple compulsory ordered mechanism at least for pig heart m-MDH might include more complex intermediates of the sort described by a reciprocating system.

A large number of physiological and nonphysiological compounds affect the activity of m-MDH and are reviewed by Banaszak and Bradshaw (20). Some studies in this thesis involved the effects of the modifier, palmitoyl-CoA, which is reviewed next. Because of its apparent non-specificity the regulatory significance of palmitoyl-CoA inhibition has been questioned. However, after a systematic study Kawaguchi et al. (26, 27) concluded that the inhibition is specific and physiologically significant. It was found that the degree of inhibition varied widely from enzyme to enzyme and those enzymes most severely affected are involved directly or indirectly in lipid biosynthesis. Comparison of inhibition by Na^+ dodecyl-SO_4, which is an indiscriminate detergent, to that by palmitoyl-CoA led to the conclusion that palmitoyl-CoA inhibits MDH and GDH in a controlled manner that may be of physiological importance. The K_i value for palmitoyl-CoA inhibition of OAA reduction by pig heart m-MDH is 1.8 μM. The inhibition is readily reversible. Palmitoyl-CoA does not alter the quaternary structure, and binds only weakly to the enzyme. Sodium dodecyl sulfate dissociates the dehydrogenase to monomeric subunits in contrast to the more selective effects of palmitoyl-CoA.

Fahien et al. (10, 13) found that GDH and to a smaller extent CS protects MDH from inhibition by palmitoyl CoA. MDH and GDH associate with each other only weakly if at all in the absence of palmitoyl-CoA.

CS is much less efficient than GDH in protecting MDH from palmitoyl-CoA inhibition (10). GDH could protect when palmitoyl-CoA was at a 3000 molar excess to GDH. CS cannot protect in the presence of greater than 100-fold molar excess palmitoyl-CoA to CS. It is not clear by which mechanism CS protected MDH. Possibly at the high palmitoyl-CoA concentrations CS bound MDH as GDH does. Alternatively, since CS binds to the order of 20 palmitoyl-CoA/CS (28) it may have simply lowered the effective palmitoyl-CoA concentration below that which inhibits MDH.

Citrate Synthase

Citrate synthase (29) catalyzes the first reaction of the citric acid cycle:

$$\text{Oxalacetate} + \text{acetyl-CoA} + H_2O \rightleftharpoons \text{citrate} + \text{CoA} + H^+ \qquad (1\text{-}3)$$

It seems probable that the enzyme *in vivo* catalyzes the reaction in one direction only - toward citrate synthesis. CS, exclusively a mitochondrial enzyme in eukaryotes, is found in all aerobic cells that have been examined, and has been isolated from animal, plant and microbial sources. Eukaryotic citrate synthase has a molecular weight of 100,000 and is dissociable into two inactive physically indistinguishable subunits. Pig heart citrate synthesis consists only of amino acids. It has no prosthetic group and requires no metal ions for activity. The enzyme possesses six to eight sulfhydryl groups, which appear to be occupied in internal hydrogen bonding to maintain the proper conformation of the active site. The active site appears to be devoid of sulfhydryls. The activity of pig heart CS is inhibited by monovalent

cations in the decreasing order $Li^+ > K^+ > Na^+ > Cs^+$, and thiocyanate, and by Mg^{2+}, ATP, and palmitoyl-CoA. The enzyme is situated at the entry to the citric acid cycle and ATP, a citric acid cycle end product, is believed to be a feedback regulator. The physiological significance of palmitoyl-CoA control is questionable. The reaction mechanism is well worked out and described in detail in the review of Spector (29).

Summary of Rationale and Objectives

Polymer "incompatibilities" causing liquid-liquid phase separations are prevalent and extensively documented (3). Recently studies show that polymers such as PEG and dextran can also induce or enhance protein associations and precipitations. For example, Halper and Srere (11) found that PEG precipitated a heterologous complex of MDH and CS. Experimental and theoretical evidence indicate that polymer interactions are the common cause of these phase separation and protein association effects. Thus, the ultimate goals of our research are to clarify the effects of physiological polymers and their mixtures on enzyme associations and catalytic properties. A specific goal of this thesis research was to determine the extent and nature of PEG effects on MDH and CS enzymes in solution; i.e., effects at lower PEG concentrations than those causing the enzyme precipitations. Questions studied were: 1) Do the enzyme associate and what factors influence this association? 2) Do the complexes consist of self-associated or cross-associated associated proteins in the MDH, CS mixture? 3) Does a major enzyme fraction polymerize? 4) What are the kinetic properties of a MDH-CS complex?

Anomalous kinetics of the coupled AAT and MDH reactions in the

absence of polymers had been reported (1), which implied anomalous kinetics of all OAA coupled enzymatic reactions. Thus, it was necessary to clarify these possible anomalies before polymer effects on enzyme kinetics could be evaluated. Bryce et al. used two independent methods: measuring lag times and isotope ratios to indicate the kinetic anomalies. However, Manley et al. (2) were unable to find any anomalous lag-transients. Also, the model proposed by Bryce et al. did not reasonably explain their isotope results. Therefore, the isotope experiments and their analysis were investigated in this thesis research.

CHAPTER II

EXPERIMENTAL

Materials

DTP, Sepharose CL-6B-200 resin, PEG (20,000), CNBr activated Sepharose 4B resin, N^6-[6-Aminohexyl)carbamoylmethyl]-ATP, Sephadex G-50 resin, NAD^+, Porcine CS, palmitoyl-CoA, DTNB, Coenzyme-A, m-MDH, OAA, L-malic acid, and Dowex resins (AG-1-X8 and AG-50W-X8) of 200-400 mesh were from Sigma Chemical Co. INSTA GEL® scintillation fluid was from Packard Instrument Co. L-Aspartic acid and ethanolamine were obtained from Eastman Organic Chemicals, α-ketoglutamate was from Calbiochem, [^{14}C]aspartic acid (193 Ci/mol) from New England Nuclear (Boston, Mass.), and PEG (6000) was from Matheson, Coleman and Bell. Porcine cytosolic aspartate aminotransferase was prepared in Dr. David E. Metzler's laboratory. All other reagents were of analytical grade. From enzymatic assays the unlabeled aspartate (30) and malate (31) were found to be free of impurities within experimental error (approximately 2%). The [^{14}C]aspartate was purified and tested as described under Isotope Incorporation, Experimental.

Methods

Dynamic Light Scattering

Theory. Dynamic light scattering data are basically the autocorre-

lated fluctuations of the intensity of scattered light. In the experiments a monochromatic beam of laser light impinges on a sample. This electric field of light induces an oscillating polarization of electrons in the molecules. The molecules then serve as secondary sources of light and subsequently radiate (scatter) light of the same wavelength as the incident light. This light is scattered into a photomultiplier placed at an angle θ with respect to the transmitted beam.

The instantaneous intensity of this scattered light depends on the instantaneous positions and momenta of all the particles in the scattering volume, since destructive interference of the scattered light depends on intermolecular distances between the light scattering particles. By virtue of their thermal motions the particles are constantly jostling around so that their positions and momenta are changing in time - thus, so is the scattered light intensity. These fluctuations of intensity make the intensity signal, $A(t)$, versus time look like random noise.

The intensity, $A(t)$, at time, t, is 'autocorrelated' with the intensity at time, $t + \tau$. The autocorrelation function of the intensity property A is defined by (32):

$$G(\tau) = \lim_{T \to \infty} \frac{1}{T} \int_0^{(T)} dt A(t)A(t+\tau) \qquad (2\text{-}1)$$

The measured autocorrelation function, $G(\tau)$, is a function of the diffusion coefficients of the scattering particles. For a mixture of N different types of particles (33),

$$G(\tau) = \left(\sum_{i=1}^{N} I_i \exp^{-\Gamma_i \tau} \right)^2 + B \qquad (2\text{-}2)$$

where

I_i = a weighting factor proportional to the intensity of the light scattered by the i^{th} species

B = a factor proportional to the average scattering intensity

$$\Gamma_i = K^2 D_i \qquad (2\text{-}3)$$

D_i = the translational diffusion coefficient of particle of type $\underline{i}$

$$K = \frac{4\pi\eta_o}{\lambda} \sin^2 \frac{\theta}{2} \qquad (2\text{-}4)$$

λ = wavelength of light transmitted in vacuum

η_o = solvent index of refraction (1.33 for H_2O)

θ = angle of photomultiplier with respect to the transmitted beam.

For a monodisperse system:

$$G(\tau) = (I \exp^{-\Gamma_i})^2 + B \qquad (2\text{-}5)$$

Nonlinear least squares fitting of Equation (2-5) to experimentally determined $G(\tau)$ values will provide the best fit value of Γ and, therefore, D using Equations (2-3) and (2-4). For a polydisperse system there are at least three approaches to obtaining diffusion coefficients from experimental data. One approach is to presuppose a specific form for the distribution of molecular sizes and obtain diffusion coefficients from Equation (2-2). Two approaches do not

require prior knowledge of the distribution: the method of cummulants (34) and the histogram method (35). The cummulant method works best with narrow distributions. The histogram method can be applied to moderately broad and/or bimodal particle size distributions.

Experimental. Samples were passed through 0.45 μm filters into Phoenix T-108 light scattering cells that had been flushed with dust-free water. The Millipore filter holders were also prerinsed with dust-free H_2O. One ml of a PEG solution was first filtered into the cell, followed by filtering one ml of the solution containing enzymes directly into the same cuvette. Mixing was by gentle stirring with a small magnetic stirring bar to avoid introduction of air bubbles. This method gave particle free blanks, The light scattering photometer, assembled by Dr. Ackerson in our Physics Department ,36, used a 15 mwatt spectra Physics continuous helium-neon laser and an ITT FW 130 photo-multiplier tube set at a 90° scattering angle. The sample was partially immersed in a water bath for temperature control. The photomultiplier was interfaced to a Langley-Ford digital correlator which autocorrelated the light intensity fluctuations. The correlator was interfaced to a PDP 11/10 computer for storage of data on disk. The data was examined by the method of cummulants which yields the z average diffusion coefficient.

Chemical Cross-linking of Enzymes Followed by Gel Chromatography

Chemical crosslinking of enzymes was attempted by adding 2 mg of DTP to 2 ml of a gently stirring protein solution (55 μg) in 27.5 mM

potassium phosphate buffer, pH 7.5. The reaction was allowed at least three hours at room temperature to go to completion. A 0.5 ml aliquot of the mixture was diluted to 1 ml with 100 mM potassium phosphate buffer, pH 7.5 and applied directly to a 7.7 cm x 2.5 cm column of Sepharose, CL-6B-200 gel. The column was equilibrated and eluted with the 100 mM potassium phosphate buffer. The elution was monitored by assaying fractions for MDH and CS activity.

The mixture containing PEG (20,000) was not added directly to the Sepharose column. The presence of even the small amount of high molecular weight polymer retarded the elution of protein so that separation of different molecular weight fractions was not possible. Instead the mixture was applied to a 1.3 cm x 1.9 cm affinity column of Sepharose 4B[N^6-(6-aminohexyl)carbamoylmethyl]ATP packed gel (see ATP-Sepharose Affinity Chromatography). The CS was bound and PEG washed off with 20 ml of 5 mM potassium phosphate, pH 7.5 buffer. CS was desorbed by a 1 ml pulse of 100 µM OAA and 1 mM CoA, and eluted in 7 ml of the 5 mM potassium phosphate buffer. Three ml of the eluted CS was then added to the Sepharose column.

The percentages of high molecular weight or cross-linked material were calculated by plotting the activities in the void volume peak and the major peak on appropriate scales then cutting out and weighing the graphed peaks to determine the relative areas.

Standard Enzyme Assays and Protein Concentration Determinations

MDH was assayed by monitoring A_{340} versus time spectrophotometrically after addition of MDH. The assay mixture consisted of 50 µM

OAA, 200 μM NADH, and 100 mM potassium phosphate buffer, pH 7.5 at room temperature. CS was assayed by monitoring A_{412} versus time spectrophotometrically after addition of CS. The assay mixture consisted of 200 μM DTNB, 500 μM OAA, 0.1 mM acetyl-CoA, and 100 mM potassium phosphate buffer, pH 7.5 at room temperature. Acetyl-CoA was prepared from CoA by the following procedure (37). CoA was dissolved in 0.1 M $KHCO_3$ to make 10 mg CoA/ml $KHCO_3$ solution. Then 1.2 μl of acetic anhydride was added per ml of CoA solution. The reaction goes to completion quantitatively producing acetyl-CoA after incubation on ice for three hours. One enzyme unit is the production of one μmol product/minute using absorptivities, ε = 6.22 mM^{-1} cm^{-1} for NADH and ε = 13.6 mM^{-1} cm^{-1} for DTNB. The enzymes, MDH and CS, in the $(NH_4)_2SO_4$ suspension were prepared by Sephadex G-50 gel chromatography. Their concentrations were determined from A_{280} measurements using ε = 0.25 mg/mg•cm^{-1} for MDH, and 1.78 mg/mg•cm^{-1} for CS.

ATP-Sepharose Affinity Chromatography

The ATP-Sepharose affinity column was prepared by coupling the ligand, N^6-[(6-Aminohexyl)carbamoylmethyl]-ATP to CNBr activathd Sepharose by the following procedure (38, 39).

CNBr activated Sepharose 4B (1.1 g) was washed with 200 ml of 1 mM HCl in several aliquots. The N^6-[(6-aminohexyl)carbamoylmethyl]-ATP (10 mg) was dissolved in 6 ml of 0.1 M $NaHCO_3$, pH 8.4. The CNBr activated Sepharose 4B was suspended in this mixture and coupling was allowed to proceed for 14 hours at 4°C with occasional stirring. The uncoupled ATP analog was removed by washing the gel on a Buchner

funnel with 200 ml of the same $NaHCO_3$ solution. The gel was then suspended in a 1 M ethanolamine solution, pH 9, for two hours at room temperature to block excess reactive sites on the CNBr activated gel. The coupled product was then washed to remove traces of noncovalently adsorbed materials. Four or five washing cycles - each cycle consisting of H_2O, followed by 1 M NaCl - were sufficient.

A 1.3 x 1.9 cm column containing this ATP-Sepharose packed gel was equilibrated with 5 mM potassium phosphate buffer at pH 7.5 before binding MDH and/or CS in the same buffer. Too high a buffer concentration, e.g. 100 mM potassium phosphate, prevents the enzymes from binding.

Sedimentation Velocities

Enzymes were sedimented by a Beckman Model E Analytical Ultracentrifuge using a Beckman AN-D rotor and the Schlieren or U.V. optical systems. Synthetic boundary experiments were made as described by Chervenka (40) with a 12 mM, charcoal-epon capillary type centerpiece. Sapphire windows were used for the Schlieren experiments. For U.V. runs the upper window was replaced with a quartz half-plane, half-wedge window and the methods described in the Beckman Technical Bulletin No. 6124 of May 1962 were used. The cells were torqued to 170 or 130 inch-lbs for Schlieren or U.V. runs, respectively. The centerpiece reference and sample sectors contained 0.45 ml and 0.15 ml, respectively. Samples were centrifuged at 50,740 RPM and Schlieren photographic plates were measured on a Nikon projector and micrometer. Densities of U.V. photographs were measured on an Auto Scanner Flur-Vis from Helena Laboratories. Sedimentation velocities were calculated by

linear regression and corrected to standard temperature and viscosity (40). The viscosities were measured with a Cannon Ubbelohde Viscometer with a H_2O drain time of 20.4 s at 25°C, viscosity range of 10-50 centistokes.

MDH Kinetics

Steady state kinetic parameters were obtained with a Durrum-Gibson stopped-flow spectrophotometer using 340 nm light and a cell of 1.86 cm path length at 25°C. The detector output, representing the solution transmittance, was digitized by a Biomation 805 A/D converter and stored in a PDP 11/40 computer for subsequent analysis. The output was collected until the reaction went to completion. These progress curves were analyzed by the CRICF computer program (41) which provides non-linear least-squares fitting of the numerically integrated rate equations to the data. In the measurements both syringes contained 27.5 µg/ml CS and/or 27.5 µg/ml MDH, 27.5 mM potassium phosphate, pH 7.5 and PEG. Syringe one contained NADH or NAD^+ and syringe two contained malate or OAA. In order to obtain all six kinetic constants from the data, progress curves with different initial concentrations of substrates and products were obtained as follows: 50 µM NADH, 50 µM OAA; 50 µM NADH, 5 µM OAA; 5 µM NADH, 50 µM OAA; 1 mM NAD, 1 mM malate, 1 mM NAD, 50 µM malate; and 50 µM NAD, 1 mM malate. These data gave good resolution of constants: V_m for OAA reduction, K_{OAA}, K_{NADH}, V_m for malate oxidation, K_{MAL}, and K_{NAD}.

The palmitoyl-CoA inhibition of OAA reduction was measured after incubating palmitoyl-CoA with the enzyme(s) in PEG for a designated amount of time. Then immediately before the measurements NADH was

added to syringe 1 and OAA was added to syringe 2 to make 50 μM NADH and 50 μM OAA in the mixed solutions. Both syringes contained the mixture of enzyme(s), PEG and palmitoyl-CoA.

Lag Time Measurements

Theory. The formation of the second product, P, in two coupled enzyme reactions follows, Equation (2-12)

$$[P] = vt + \frac{v}{k}(e^{-kt} - 1), \qquad (2\text{-}12)$$

as long as the velocity, v, of the first reaction is constant and the concentration of the intermediate, B, is low enough for the second reaction to be first order with respect to B (62). The rate constant $k = V/K_B$ where K_B and V are the Michaelis and maximal velocity constants of the second enzyme. Graphically this behavior can be observed as a lag-transient before the rate of product formation reaches the velocity v. At the lag-time, $\tau = 1/k$, the observed reaction velocity is $(1-e^{-1})v$. Summarizing, we have

$$\tau \equiv 1/k = K_B/V, \qquad (2\text{-}13)$$

which predicts the lag-time of coupled enzyme reactions from the rate constants of the second enzyme. The lag time observed graphically should agree with the lag-time calculated from Equation (2-13) from data on the individual enzymes, unless the simultaneous presence of both enzymes alters their kinetic properties. Conversely, disagreement between predicted and observed lag-times indicates altered kinetic constants in the enzyme mixture.

Experimental. For the coupled MDH and CS reactions investigated for this thesis reaction (2-14) was measured.

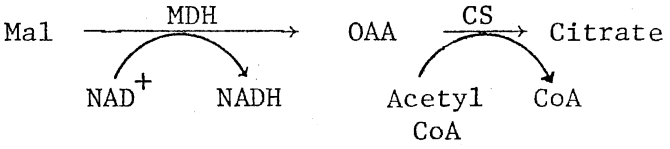

(2-14)

In theory the reverse of this reaction could be used; but, in practice the reaction equilibrium lies too far to the right for any reasonable amount of malate production. An additional reaction, required to detect CoA production, was the reaction of DTNB with CoA to produce a chromophore with λ_{max} = 412 nm. The resulting reaction sequence and kinetic constants were:

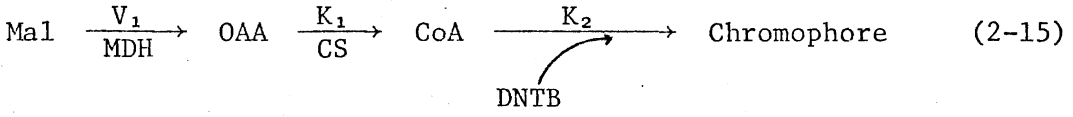

(2-15)

where V_1 is the velocity of malate oxidation, K_1 is the first order rate constant of the CS reaction and K_2 is the pseudofirst order rate constant for CoA utilization which equals K_2' [DTNB]. This thrid reaction also has a lag time:

$$\tau_2 = 1/(K_2' \text{ [DTNB]}) \qquad (2\text{-}16)$$

and the concentration of DTNB needs to be increased to keep τ_2 much shorter than the lag time we were interested in measuring,

$$\tau_1 = 1/K_1 \qquad (2\text{-}17)$$

To reduce excessive absorbance of DTNB, a wavelength of 450 nm was used for detection. The constant K_2' was measured so that a minimum DTNB

concentration necessary to make $\tau_2 << \tau_1$ could be calculated. At room temperature in 10 mM potassium phosphate buffer, pH 7.5, K_2' was found to be 0.099 sec^{-1} mM^{-1} DTNB. Constant K_2' was calculated from the pseudo first order rate constants K_2 at a known concentration of DTNB. The rate constants K_1 and K_2 were determined from first order plots of the progress curves of the reactions (using low OAA concentrations).

$$\text{OAA} \xrightarrow[K_1]{\text{Acetyl CoA}} \text{CoA} \qquad (2\text{-}18)$$

$$\text{CoA} \xrightarrow[K_2]{\text{DTNB}} \text{Chromaphore} \qquad (2\text{-}19)$$

The coupled enzyme reactions were started by adding MDH to a mixture of malate, NAD^+, acetyl-CoA and CS and monitoring the change of absorbance at 450 nm. The observed lag time, τ_{obs}, was measured graphically from the progress curve. The predicted lag time, $\tau_{pred.}$, was calculated from K_1 (Equation (2-17)).

Isotope Incorporation, Experimental

The Durrum stopped-flow spectrometer with a Model D-132 Multi-Mixing accessory was used for the experiments to measure isotope incorporation from [^{14}C]aspartate to malate at 25°C. Activities of the enzymes were determined just prior to the isotope incorporation experiments using the same instrument in the stopped-flow mode. For this purpose, the quenching solution was replaced with substrate solution and the transmittance at 340 nm measured from the stopped-flow cuvette contained in this accessory. Substrate concentrations of the reaction mixture were the same as used in the isotope incorporation

experiments except that variable oxaloacetate concentrations were used for dehydrogenase assays to permit calculation of V_m from a Lineweaver-Burk plot. An 11:1 ratio of dehydrogenase to aminotransferase units (previously demonstrated to be adequate) was used to measure the velocity of AAT catalyzed reaction, v. For isotope incorporation measurements, chemical quenching was used and the reaction time determined by the method of Bryce et al. (1). The same reaction time was also calculated from the flow velocity and flow tube dimensions. A constant flow velocity during the collection of reaction products was verified by the velocity transducer output. The composition and distribution of solutions in the stopped-flow drive syringes are given in the legend to Figure 10. Contents from three shots were collected and combined for analysis. On each shot the system was purged with 1 ml of quenched reaction mixture prior to collecting the remaining solution containing 8 ml reaction mixture and 8 ml of 0.44 M $HClO_4$ (0.22 M after mixing).

The combined reaction mixture was neutralized with KOH, the precipitated $KClO_4$ removed, and the solution made 0.1 N in HCl. This acid solution was applied to a 1.2 x 16.5 cm column of cation exchange resin (Dowex AG-50W-X8, 200-400 mesh) in the H^+ form at room temperature (25°C) and the unbound counts, containing oxaloacetate and malate, were washed off with 90 ml of 0.1 N HCl. The radioactive eluate was neutralized and applied to a 2.2 x 7.0 cm column of anion exchange resin (Dowex AG-1-X8, 200-400 mesh) in the Cl^- form at room temperature and eluted with a linear gradient made from 850 ml each of H_2O and 33 mM HCl. Elution of malate was achieved in about 1.5 hr. A column of the same dimensions as used by Bryce et al. (38) was initially used, but abandoned because

of the slow flow and long elution times from it. Resolution of radioactive peaks was slightly better on the faster column although the bed volume was the same. Malate in the column eluate was determined by the method of Hummel (43) except that the solutes were collected by evaporation of solvent with a stream of N_2 gas at room temperature instead of by Ca^{2+} precipitation and decantation. This modification gave more precise standard curves. All radioactivity was counted in 10 ml INSTA GEL® in a Beckman LS 3150 T liquid scintillation counter.

Prior to the isotope incorporation experiments, the [^{14}C]aspartate was purified and tested as follows. First the commercial [^{14}C]aspartate in 0.1 N HCl was subjected to the first chromatographic step of the isotope incorporation experiments. Unbound counts (radioactive impurities) were washed off the cation exchange column with 0.1 N HCl. Aspartate was then eluted with 1 N HCl and the eluate flash evaporated to dryness. Radioactivity from this purified aspartate was completely retained at pH 1.0 on the cation exchange column described above when subsequently tested. Secondly the coupled transaminase-dehydrogenase reaction velocity was measured using the [^{14}C]aspartate as in the isotope incorporation experiments. The same reaction velocity was obtained as with unlabelled aspartate, demonstrating that impurities in the [^{14}C]Aspartate were not affecting the transaminase activity.

CHAPTER III

RESULTS AND DISCUSSION

Evidence for PEG Induced Formation of Soluble Complexes

The first question investigated in this thesis was: do the enzymes in an MDH, CS, PEG mixture associate to form soluble enzyme complexes? Halper and Srere's study (11) showed that a high concentration of PEG will induce formation of a large amount of precipitated complexes consisting of MDH bound to CS. When the PEG concentration is lowered below the critical concentration, the enzyme mixture becomes soluble as seen by the lack of turbidity. We lowered the PEG concentration in a mixture of MDH and CS so that the enzymes were not precipitated and tested whether complexes were still being formed. Two methods, dynamic light scattering and gel chromatography, were used to detect if particles existed with sizes greater than the monomeric enzyme size. Each method detected enormous particles in solutions with PEG concentrations well below that which causes precipitation. The results will be discussed in detail in the following two sections.

Dynamic Light Scattering

DLS data, gathered at various times after mixing enzymes with 10% w/v PEG were analyzed to obtain associated enzyme average

diffusion coefficients (Figure 1A). Since diffusion coefficients are inversely proportional to size, Figure 1A shows that after an initial fast association particles slowly grow to stable sizes. Electron microscope studies by Dr. Merz of our lab (44) indicate that the enzyme complexes are spherical and exist in a broad distribution. Calculations based on the diffusion coefficients of the time stabilized particle indicate that these spherical particles may be on the order of 10^7 times the monomer size. Dr. Manley and James Appleman of our lab analyzed the DLS data of a solution identical to that described in Figure 1A except that it contained 1% rather than 10% PEG. This low concentration of PEG also induced formation of complexes, which were on the order of 500 monomers/complex, assuming a spherical shape (45).

Gel Chromatography

We first attempted to estimate molecular sizes of associated enzymes by gel chromatography of a mixture of MDH and CS on columns equilibrated with PEG. The presence of PEG is of course necessary to maintain the associated enzyme complexes. However, dextran, agarose, and acrylamide based gels (Sephadex G-200, Sepharose CL-6B, Biorad P-200) behave aberrantly in both PEG and dextran ("polymers") solutions. They do not swell to the full volume attained in polymer free buffer. Also, when enzymes are applied to the gels equilibrated with polymer, they are retained in the stationary phase. The solution to this problem was to cross-link the enzyme complexes formed in the enzyme, PEG mixture, and apply an aliquot of this mixture to a gel column equilibrated in buffer. Formation of covalent bonds between enzymes

Figure 1. Diffusion Coefficients (D) Versus Time After Mixing

A) Enzymes with PEG alone.

B) Enzymes with PEG plus substrates: 4 mM NAD^+, 8 mM OAA, and 4 mM CoA (o). Enzymes plus 20 μM palmitoyl-CoA (●).

All three solutions contained 0.2 mg/ml CS, 0.2 mg/ml MDH, pH 7.5, 5 mM potassium phosphate buffer, and 10% w/v PEG (6000) at 5°C.

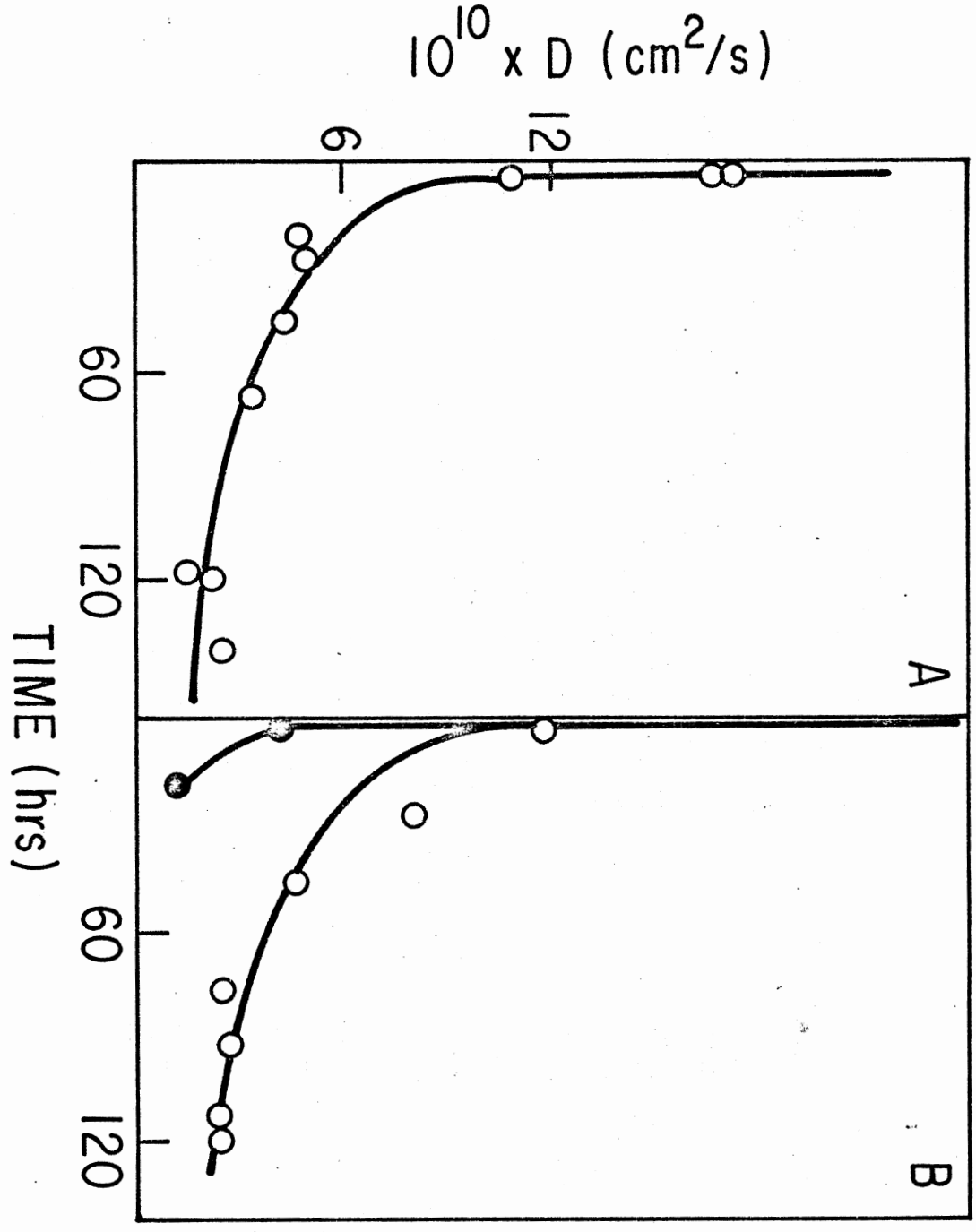
10^{10} x D (cm^2/s)
6
12
TIME (hrs)
60
120
A
60
120
B

in the complexes then prevented the complexes from dissociating in the buffer environment.

The cross-linking agent selected was a bifunctional imidate, DTP, which stabilized complexes formed in an enzyme, PEG mixture; however, the conditions had to be changed slightly from Halper and Srere's in order for this reagent to be reactive. So, before presenting the gel chromatography results, we show that the specific interaction between MDH and CS, observed by Halper and Srere, also occurred under these conditions of higher temperature and higher buffer concentration. Table II shows that 25% PEG does not precipitate MDH or CS alone; however, when the two are mixed precipitation occurs as indicated by its turbidity and increased optical density. The increased total protein concentration did not cause this precipitation, as each enzyme at concentrations less than 0.1 μM could not possibly affect the solubility of the other by long range interactions or by altering the solvent surrounding other molecules. The most reasonable explanation is that MDH and CS form a new species, a heterologous complex which is less soluble than either enzyme alone.

In all of the following tests which involved cross-linking, the conditions were the same as described in Table II; that is 27 mM potassium phosphate, pH 7.5, and room temperature. Figure 2 shows elution profiles of enzyme mixtures treated with DTP in the presence (Figure 2A) and absence (Figure 2B) of PEG. Only in the former case does any enzyme elute in the void volume, indicating enzyme complexes of 4×10^6 daltons or larger - greater than 40 times the monomeric enzyme size.

The possibility existed that the high molecular weight fractions

TABLE II

PRECIPITATION OF MDH AND CS BY PEG

Enzyme(s)	A_{600}	Appearance
MDH	0.00	Clear
CS	0.00	Clear
MDH plus CS	0.11	slightly turbid

Solutions were 27.5 µg/ml MDH and/or 27.5 µg/ml CS in 27.5 mM potassium phosphate buffer, pH 7.5, and 25% PEG (6000) at room temperature.

Figure 2. Elution Profiles of DTP-Treated Mixtures of MDH and CS at Room Temperature. Solutions containing: 27.5 µg/ml CS (——); 27.5 µg/ml MDH (---); 27.5 mM potassium phosphate buffer, pH 7.5; and A) 2000 w/v PEG (6000), or B) no PEG were incubated with a cross-linker, 1 mg/ml DTP, and fractionated by Sepharose CL-6B gel chromatography. Elution of Blue Dextran (•••).

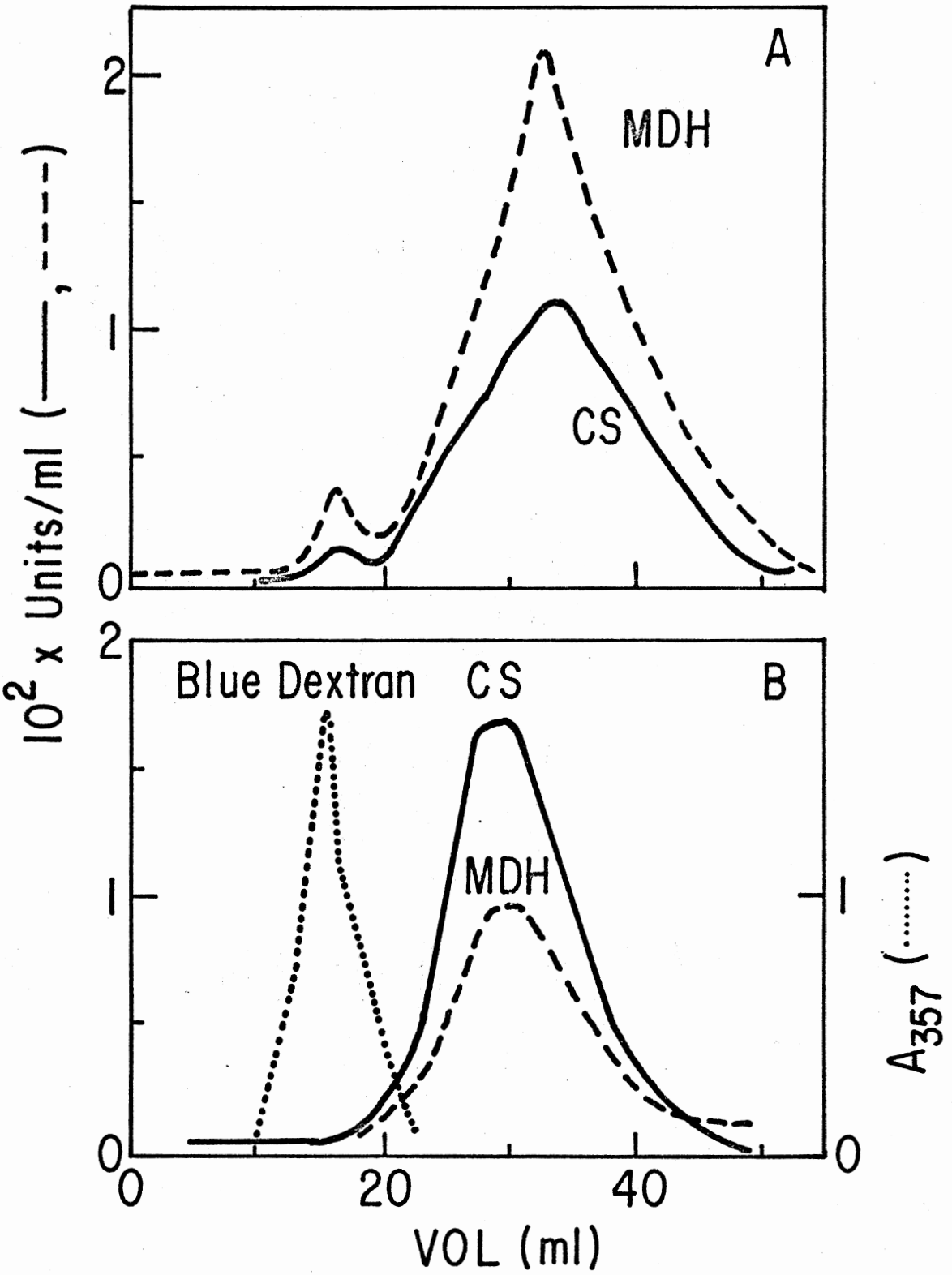
A
MDH
CS
2
1
0
10^2 x Units/ml (——, - - - -)
Blue Dextran
CS
B
MDH
2
1
0
0
20
40
VOL (ml)
1
0
A_{357} (.....)

consisted of a conglomerate of protein cross-linked to PEG rather than associated protein. This is because 20% (w/v) PEG is 22 mM compared to 0.1 μM enzyme. Therefore, the specificity of the DTP for the protein amino groups in the presence of the PEG terminal hydroxyl groups needs consideration. Hunter and Ludwig (46) tested DTP reactivity with hydroxyls. Imidoesters react with water as well as the target amino groups. Addition of small molecules, containing aliphatic hydroxyl groups, to make an 0.05 M-0.1 M solution did not increase the rate of DTP utilization over its rate of hydrolysis. So, in a solution of PEG and protein excess DTP would be hydrolyzed by H_2O before reacting with the hydroxyl groups of PEG.

Other results also indicate that DTP reacts predominantly with protein and not PEG. A three-fold increase in the molecular weight of PEG at the same weight concentration (10% w/v) caused a 20-fold increase in the fraction of enzyme found in the high molecular weight peak (Figure 4). Since the PEG hydroxyl concentration decreased from 33 mM to 10 mM, any reactivity between PEG and DTP should have decreased. However, an increase in the amount of associated protein with increasing PEG molecular weight is in agreement with the similar dependence of liquid-liquid phase separation on polymer molecular weights (3). An increase in the amount of associated protein best explains the increase of DTP reactivity. Recent experiments of Atha and Ingham (47), including equilibrium dialysis measurements, also argue against any binding of PEG with proteins.

Conditions Affecting Association

The ability of proteins to associate is sensitive to solution

conditions such as ionic strength, protein concentration, ligand binding, etc. In our system protein association is further affected by properties of the polymer such as its concentration, molecular weight, and d-gree of substitution. I found that increasing PEG concentration and molecular weight increase the extent of association as do binding of the ligand, palmitoyl-CoA. Binding of substrates appears to have no effect. These results are discussed in detail in the following sections.

Effect of PEG Concentration

After cross-linked complexes are formed in PEG, high molecular weight, associated protein will elute in the void volume of Sepharose gel (Figure 2A). Figure 3 shows that increasing PEG concentration increases the extent of this association to about the same extent in the mixture of enzymes as in solutions of each enzyme alone.

Effect of PEG Molecular Weight

Increasing the molecular weight of PEG, but keeping its total mass constant, causes a more than proportional increase in the amount of associated protein. Figure 4 shows the elution profile of DTP treated CS which had been incubated in 10% (w/v) PEG of molecular weight 6000 (Figure 4A) or molecular weight 20,000 (Figure 4B).

Effect of Ligand Binding

I tested the effects of palmitoyl-CoA and substrate binding on PEG induced association. Palmitoyl-CoA was chosen because it binds

Figure 3. Effect of PEG Concentration on Associated Protein

A) Both enzymes (27.5 µg/ml MDH and 27.5 µg/ml CS) with PEG.

B) Each enzyme alone (55 µg/ml) with PEG.

The enzymes, cross-linked by 1 mg/ml DTP in 27.5 mM potassium phosphate buffer, pH 7.5; and PEG (6000) at room temperature, were fractionated by Sepharose CL-6B-200 gel chromatography. % Enzyme in V_o = Area of Void Volume Peak/Total Elution Area.

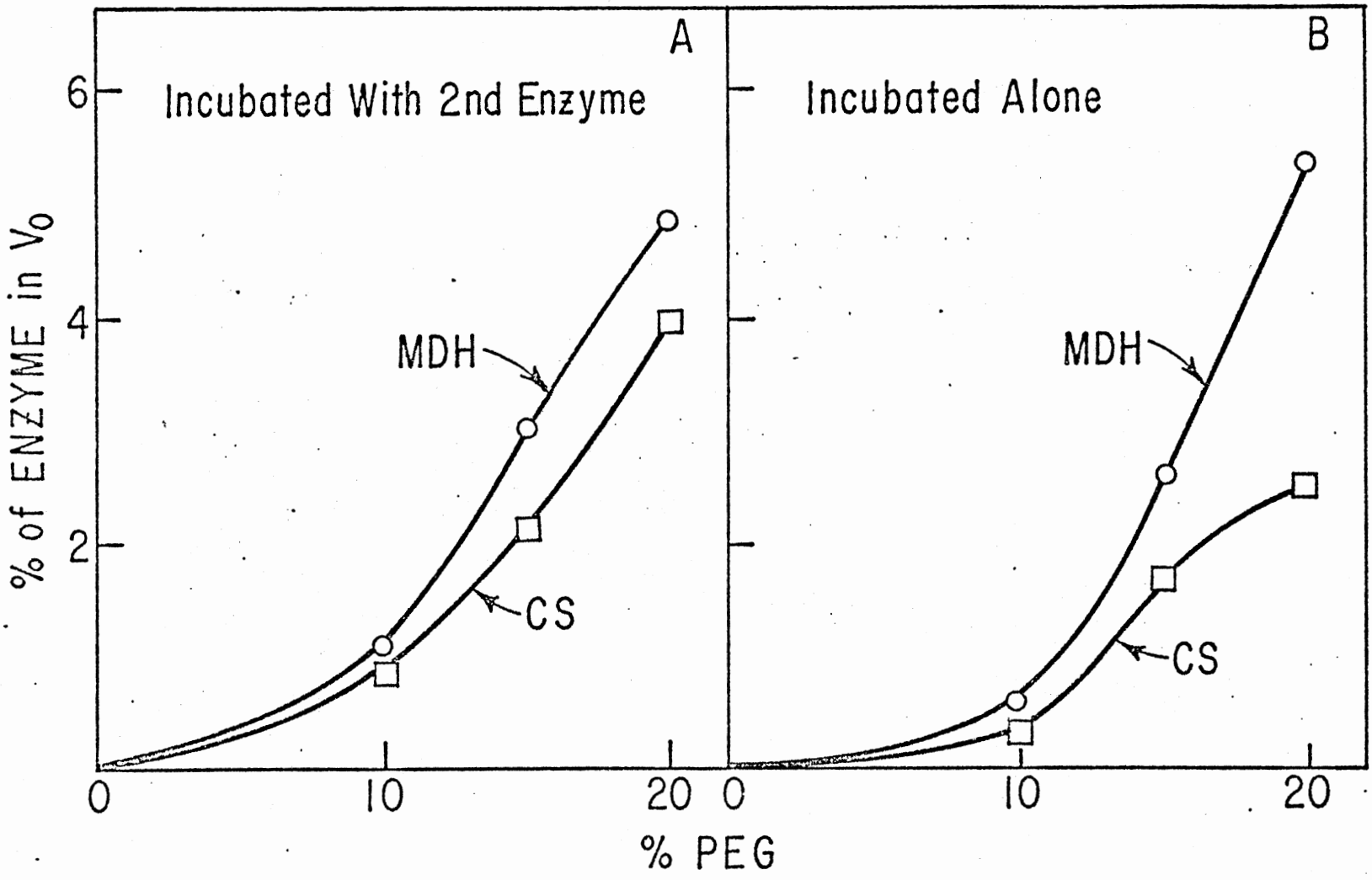
A
Incubated With 2nd Enzyme
B
Incubated Alone
6
4
2
0
10
20
% of ENZYME in V_o
MDH
CS
% PEG

Figure 4. Comparison of Associated Protein Formed in the Presence of 6000 and 20,000 Molecular Weight PEG

A) 6000 M_r PEG.

B) 20,000 M_r PEG.

Both solutions contained 55 μg/ml CS in 27.5 mM potassium phosphate buffer, pH 7.5, and 10% (w/v) PEG at room temperature. The enzymes were cross-linked with 1 mg/ml DTP, the 20,000 M_r PEG was removed from B (see Chapter II, "Chemical Cross-linking of Enzymes Followed by Gel Chromatography"), and enzymes were fractionated by Sepharose CL-6B-200 gel chromatography.

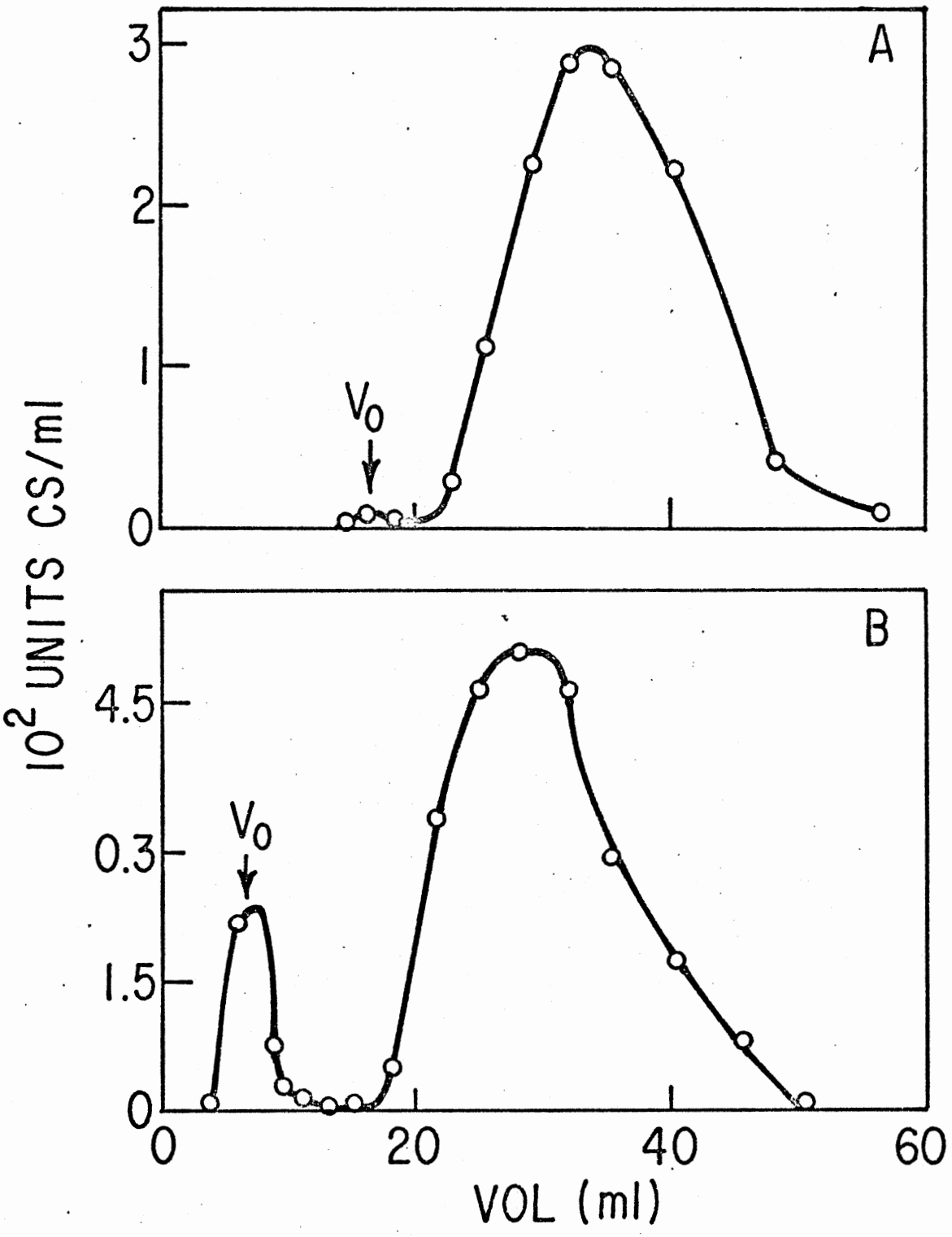
A
B
V_0
V_0
3
2
1
0
4.5
0.3
1.5
0
0
20
40
60
10^2 UNITS CS/ml
VOL (ml)

to MDH and CS and induces MDH, GDH complexation in the absence of PEG (13). Diffusion coefficients (Figure 1) obtained from our dynamic light scattering measurements show that binding of substrates to MDH and CS has little effect, whereas, palmitoyl-CoA greatly increases the size of PEG induced enzyme aggregates.

Composition of Complexes

The question next investigated was, "Are the soluble complexes primarily heterologous (made of MDH bound to CS) or are they primarily homologous (made of MDH bound to MDH and CS bound to CS)?" The following test was devised. A column packed with Sepharose bound [N^6-(6-aminohexyl)carbamoyl-methyl]-ATP (ATP-Sepharose) binds both MDH and CS. When a mixture of MDH and CS is applied to this column each can be desorbed only by its own biospecific elution condition (Figure 5B). I cross-linked enzyme complexes formed in 1% PEG, isolated these complexes by Sephadex G-200 gel chromatography, applied them to the same ATP-Sepharose column, and eluted with their specific substrates (Figure 5A). If the crosslinked complexes had consisted of a one-to-one heterologous association between both enzymes, an equal percent of the second enzyme would elute with the enzyme which was specifically being desorbed. However, specific desorption of CS with OAA + CoA pulse eluted 93% of the CS and only 2% of the total bound MDH. Desorption of MDH with the NADH pulse eluted 98% of the MDH and only 7% of the CS. These results indicate that enzyme association is primarily homologous.

Figure 5. Elution of MDH (o) and CS (□) from ATP-Sepharose Packed Affinity Column

A) MDH and CS complexes cross-linked at room temperature in 1% PEG and isolated by gel chromatography (see legend to Figure 2) were applied to the affinity column.

B) A mixture of 40 µg/ml MDH plus 40 µg/ml CS in 5 mM potassium phosphate buffer, pH 7.5 was applied to the affinity column.

At the arrows a pulse of the indicated reagents was introduced into the flow at 5°C.

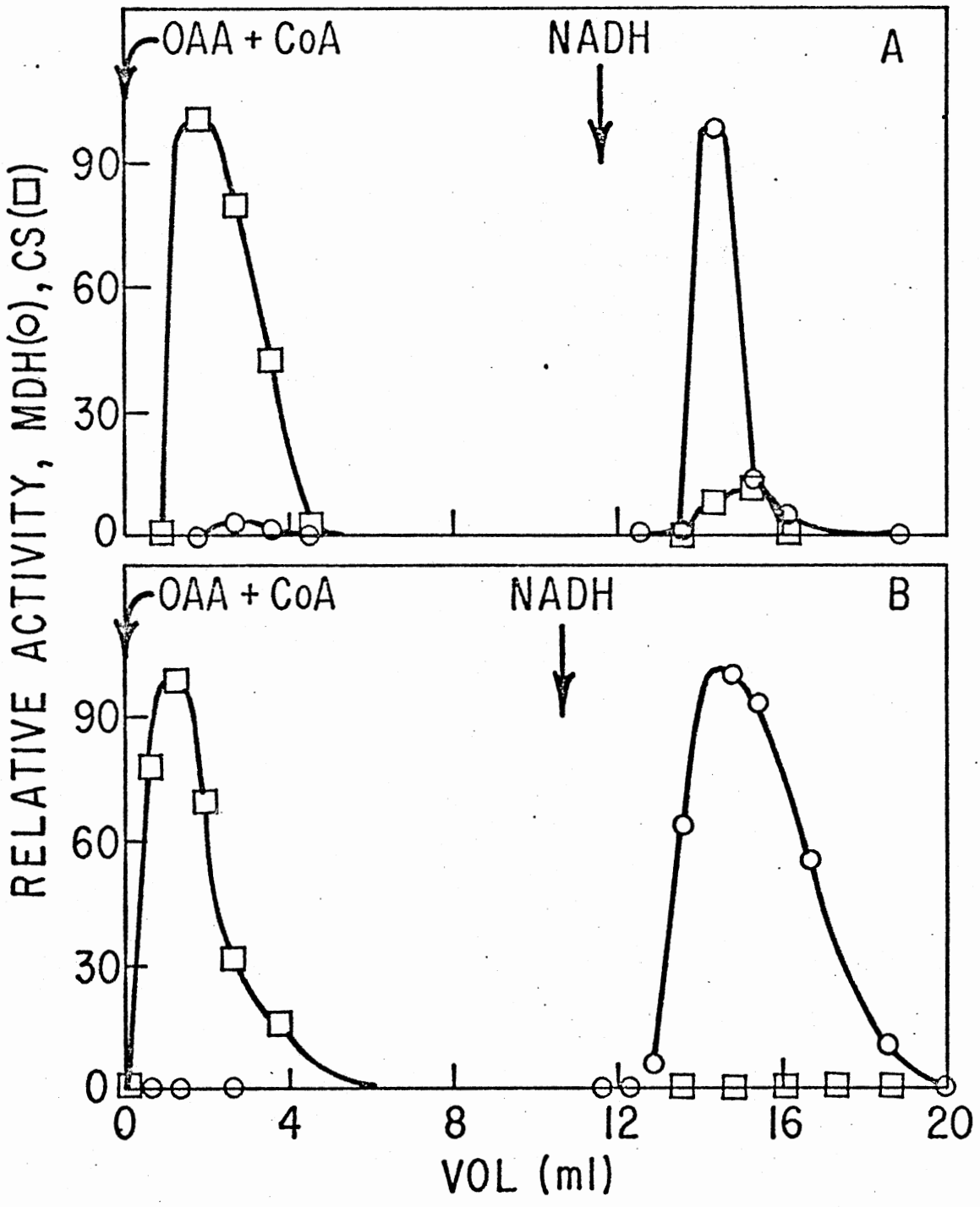
OAA + CoA
NADH
A
OAA + CoA
NADH
B
RELATIVE ACTIVITY, MDH(o), CS(□)
90
60
30
0
0
4
8
12
16
20
VOL (ml)

Fraction of Associated Enzyme

Another question investigated was "What fraction of the soluble enzymes out of the total enzyme mass becomes associated?" The following results indicate that the complexes usually consist of only a small fraction of total enzyme mass.

Binding to MDH-ATP-Sepharose Affinity Column

In this experiment I measured PEG induced binding of CS to column-bound MDH. The steps are shown in Figure 6. At the first arrow 0.08 mg of MDH was applied to the ATP-Sepharose affinity column which was equilibrated with 5 mM potassium phosphate, pH 7.5. The entire aliquot bound to the column because the next 10 ml of buffer, which was five times the bed volume, did not elute any excess MDH. The column was then equilibrated with the buffer containing 1% PEG by passing 15 ml of this solution over the column (not shown on graph). As the next arrow indicates, 0.08 mg of CS was applied to the column. It was now possible for the PEG to induce binding of this mobile equimolar, 0.08 mg CS to the 0.08 mg of column-bound MDH. However, in the next step, when the column was washed with more 1% PEG, unbound CS began to elute (Peak A). It took approximately 250 ml to elute all this CS because a PEG solution apparently causes protein to be partially immobilized in the stationary pores. (This problem is also discussed in the "Gel Chromatography" section, Chapter III). Then the PEG was washed off the column with buffer. Removal of buffer desorbs the CS bound to the column-bound MDH by virtue of a PEG induced attraction. Peak B shows that a small amount of CS had associated

Figure 6. Association of CS with Column Bound MDH. At the arrows the indicated reagents were introduced into the flow of either 5 mM potassium phosphate buffer, pH 7.5 or 1% PEG at room temperature. The 1.3 x 1.9 cm column consisted of ATP-Sepharose. Introduced into the flow from left to right were80 µg MDH in 200 µl buffer, 80 µg CS in 200 µl 1% PEG, 100 µM OAA plus 1 mM CoA in 1 ml buffer, and 1.4 mM NADH in 1 ml buffer.

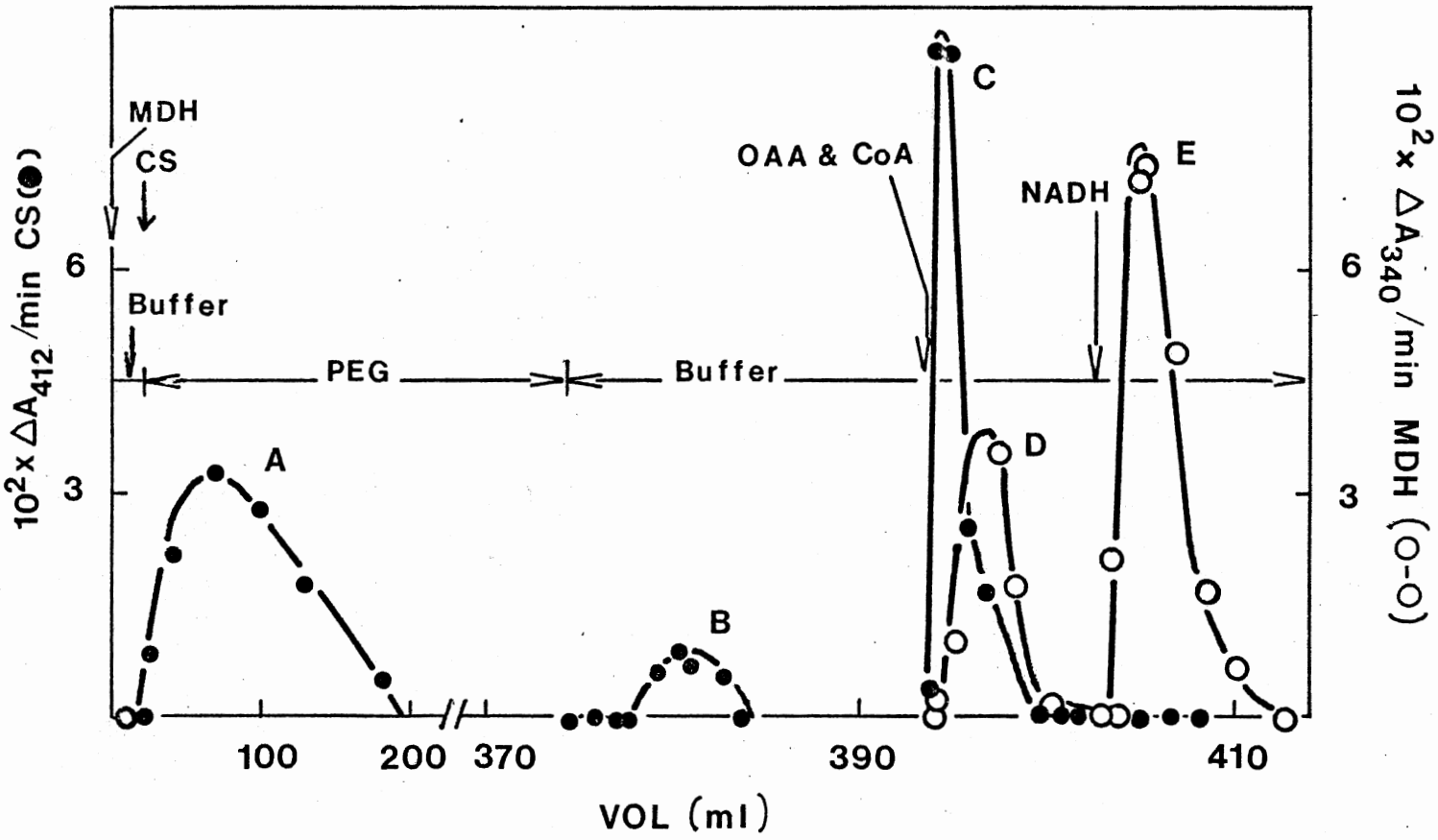
MDH
CS
Buffer
PEG
Buffer
OAA & CoA
NADH
A
B
C
D
E
6
3
6
3
100
200
370
390
410
VOL (ml)
10² x ΔA412 /min CS (●)
10² x ΔA340 /min MDH (O-O)

with the MDH. Evidently a few ATP sites were not saturated by MDH since a pulse of OAA-CoA desorbed some ATP-bound CS (Peak C). Due apparently to some irreversible effect of PEG on MDH binding to the ATP sites, some MDH was desorbed by the CS biospecific elution condition (Peak D). NADH eluted the remaining MDH and no CS (Peak E). Some quantitation can be achieved from this sequence (noting the expansion of the abscissa scale above 200 ml of eluant). Though 5% (Peak C) of the CS bound to the ATP ligands, the rest was available to associate with the equimolar column-bound MDH. However, only 1% (Peak B) bound to the MDH, while the rest (Peak A) eluted with the PEG wash, so PEG caused only 1% of a CS solution to bind to an equimolar amount of column bound MDH.

Sedimentation Velocity Measurements

Sedimentation velocity measurements on the MDH-CS-PEG system characterize the state of enzyme associations in a manner complementary to that of dynamic light scattering. Light scattering intensities are dominated by contributions from the very large molecular weight species. Thus, the aggregation of species of considerably lower molecular weight cannot be detected from our light scattering data; although, these species may represent the largest fraction of the total protein weight. The amplitude of the Schlieren peak in sedimentation velocity experiments, however, is proportional to the weight concentration of the protein irrespective of its molecular weight, and is limited in sensitivity to a few tenths of a mg of protein/ml. Thus, with a 1-2 mg/ml protein solution 10% of this protein mass could move with a greatly different velocity from the remaining 90% and never be detected. In

summary, the light scattering data characterize the most associated enzyme species and, as shown below, the sedimentation data characterize the majority of the remaining enzyme species.

The sedimentation velocity, s, observed for the MDH-CS mixture in 1% PEG was 5.64 (Table III) and the peak amplitude is close to that expected for this protein concentration. The relation between $\underline{s}$ and molecular weight is adequately constant (48) to predict that a dimer of MDH or CS molecules would have $\underline{s}$ values about 50% higher than that of the monomers. Since the $s_{20,w}$ of the mixture of MDH and CS monomers is 5.50, we conclude that the major fraction ($\geq$ 90%) of the enzyme mass is in a monomeric state with 1% PEG. The sedimentation velocity observed in the MDH-CS-1% PEG mixture with 20 μM palmitoyl-CoA and 100 μM palmitoyl-CoA was 5.89 and 8.60, respectively. Increasing palmitoyl-CoA to 100 μM apparently induces association of the majority of the enzyme. It is not known yet whether this represents homologous or heterologous association or both.

Though the sedimentation velocity results in the dilute (1%) PEG were unequivocal, problems occurred when attempting to sediment the mixture in concentrated PEG. As the concentration was increased an increasingly large band of protein did not move with the sedimenting band but remained at the boundary. In 5% PEG the Schlieren peak remained at the synthetic boundary position indicating that none of the protein was sedimenting. As shown in Table IV several conditions were changed to test for possible causes of the aberrant sedimentation behavior. Gross denaturation might cause this, and possible culprits were palmitoyl-CoA and/or a contaminant in the recrystallized PEG. So the MDH was centrifuged in a solution in which it had maximum specific

TABLE III

$s_{20,w}$ AS A FUNCTION OF PEG AND P-CoA CONCENTRATION

% PEG (6000) (w/v)	P-CoA		
	0	20 μM	100 μM
0	5.50 ± .11	5.18 ± .18	-
1	5.64 ± .03[b]	5.89 ± .24	8.65 ± .13
2	-	-	-
3	-	6.46 ± .51[a]	-
4	-	6.26 ± .53	-
5	5.38 ± .07[c]	-	-

All solutions contained 1 mg/ml MDH, 1 mg/ml CS, and 5 mM potassium phosphate, pH 7.5 at 5°C.

[a]A peak remained at the boundary.

[b]Unpublished work of E. R. Manley, pH 7.0.

[c]Experiment with UV optics and 4.0% PEG as the synthetic boundary forming solution.

TABLE IV

COMPARISON OF CONDITIONS OF SEDIMENTING AND NONSEDIMENTING PROTEINS

	Sample Solution			Synthetic Boundary Forming Solution	No. Runs	Sedimentation
COND.	Enzyme(s)	20 μM Palmitoyl-CoA	PEG			
A	MDH,CS	+	recrystallized[a]	5% PEG	2	-
B	MDH,CS	-	recrystallized[a]	5% PEG	2	-
C	MDH	-	untreated	5% PEG	2	-
D	MDH	-	untreated	-	1	+
E	MDH,CS	-	recrystallized	2.5% PEG	1[c]	+
F	BSA	-	untreated	5% PEG	1[b]	+

[a]Methods in Virology, 2, pg 303.

[b]Room temperature.

[c]Experiment used U.V. optics.

activity (COND. C) and again the enzyme remained at the boundary. This showed denaturation was not the cause. In COND. A, B, or C a solution of 5% PEG was layered on top of the protein solution containing 5% PEG to form a synthetic boundary. The protein did sediment 1) when the protein solution was centrifuged without forming a synthetic boundary (COND. D) and 2) when the PEG in the synthetic boundary forming solution (2.5% in COND. E) was less dense than the PEG in the protein solution (5% PEG). Apparently increasing the density difference between the synthetic boundary forming solution and protein solution prevents the aberration by stabilizing the synthetic boundary against mechanical and thermal convections. This problem is well documented (49) but, does not normally occur in PEG free solutions in which the protein alone provides sufficient density differences.

Some of the data then in Table III have the aberration just discussed. However, the data is consistent with the rest of the table in that in all cases the portion of enzyme which did sediment, did so as monomeric enzyme. Since 6% PEG precipitates the MDH, CS and 20 μM palmitoyl-CoA mixture and the enzymes still sedimented as monomers in 4% PEG, it appears that the complexes always contain less than 10% of the protein mass in this system.

Kinetics

We attempted to measure the kinetics of the MDH-CS heterologous complex. Though heterologous associations can cause large catalytic changes in principle, a significant fraction of the total enzyme must exist as complexes in order to detect these kinetic changes. The results up to this point indicate that only a small amount of hetero-

logous complexation takes place with PEG concentrations less than those precipitating the enzymes. Kinetic studies with such solutions, described next, corroborate this conclusion.

MDH Kinetics in the Presence and Absence of CS

The kinetic parameters for MDH were measured in the presence and absence of CS at increasing PEG concentrations. This tested whether increasing PEG concentrations could force CS to bind a large fraction of MDH and cause significant kinetic changes. Figure 7 shows the ratio of kinetic parameters with PEG to the parameter value without PEG as a function of PEG concentrations. Increasing the PEG concentration close to the point at which it precipitates the mixture (Table II) does affect MDH catalytic properties in the presence of CS (Figure 7). However, as shown in Figure 8, these same trends are found in the absence of CS. The change in kinetics of MDH alone is likely caused by the effects of PEG on the water structure. So, either little heterologous association occurred or the CS bound MDH has kinetic properties similar to MDH alone.

Lag Time Measurements

The lag time of CoA production by the consecutive reactions catalyzed by MDH and CS was measured in the presence and absence of PEG and compared to the predicted lag time. The results, summarized in Table V, show no significant difference between the measured and the predicted lag time, both in the presence and absence of PEG.

Figure 7. MDH Steady State Kinetic Parameters in the Presence of CS. The parameters were measured in solutions containing 27.5 µg/ml MDH, 27.5 µg/ml CS, 27.5 mM potassium phosphate buffer, pH 7.5 and substrates at 25°C in increasing concentrations of PEG (6000). K_{INIT} is the parameter value in the absence of PEG. V_1 and V_2 are the maximal velocities for OAA reduction and malate oxidation, respectively.

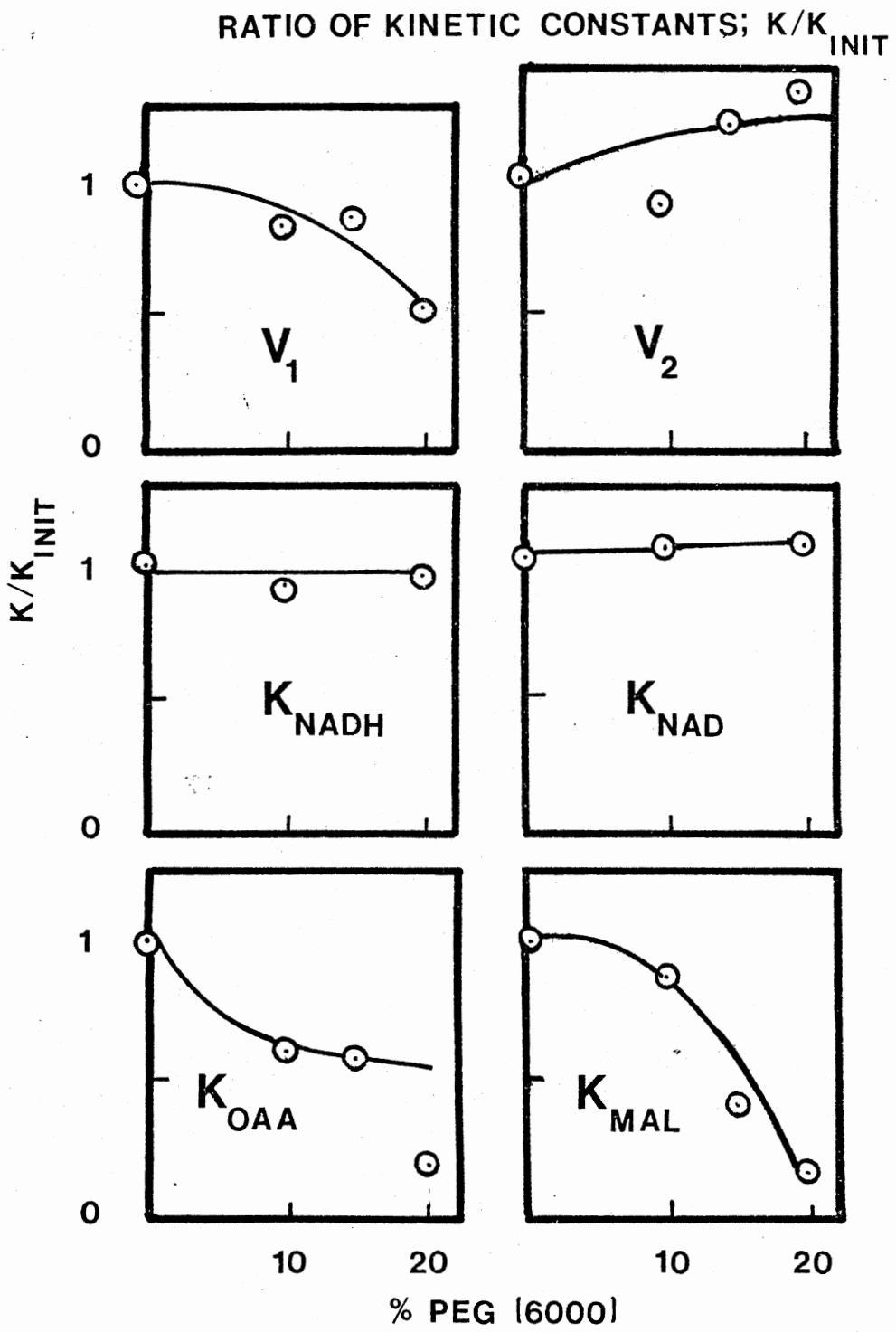
RATIO OF KINETIC CONSTANTS; K/K INIT
K/K INIT
1
0
V1
V2
KNADH
KNAD
KOAA
KMAL
10
20
% PEG (6000)

Figure 8. MDH Steady State Kinetic Parameters in the Absence of CS. The parameters were measured in solutions containing 27.5 µg/ml MDH, 27.5 mM potassium phosphate buffer, pH 7.5 and substrates at 25°C in increasing concentrations of PEG (6000). K_{INIT} is the parameter value in the absence of PEG. V_1 and V_2 are the maximal velocities for OAA reduction and malate oxidation, respectively.

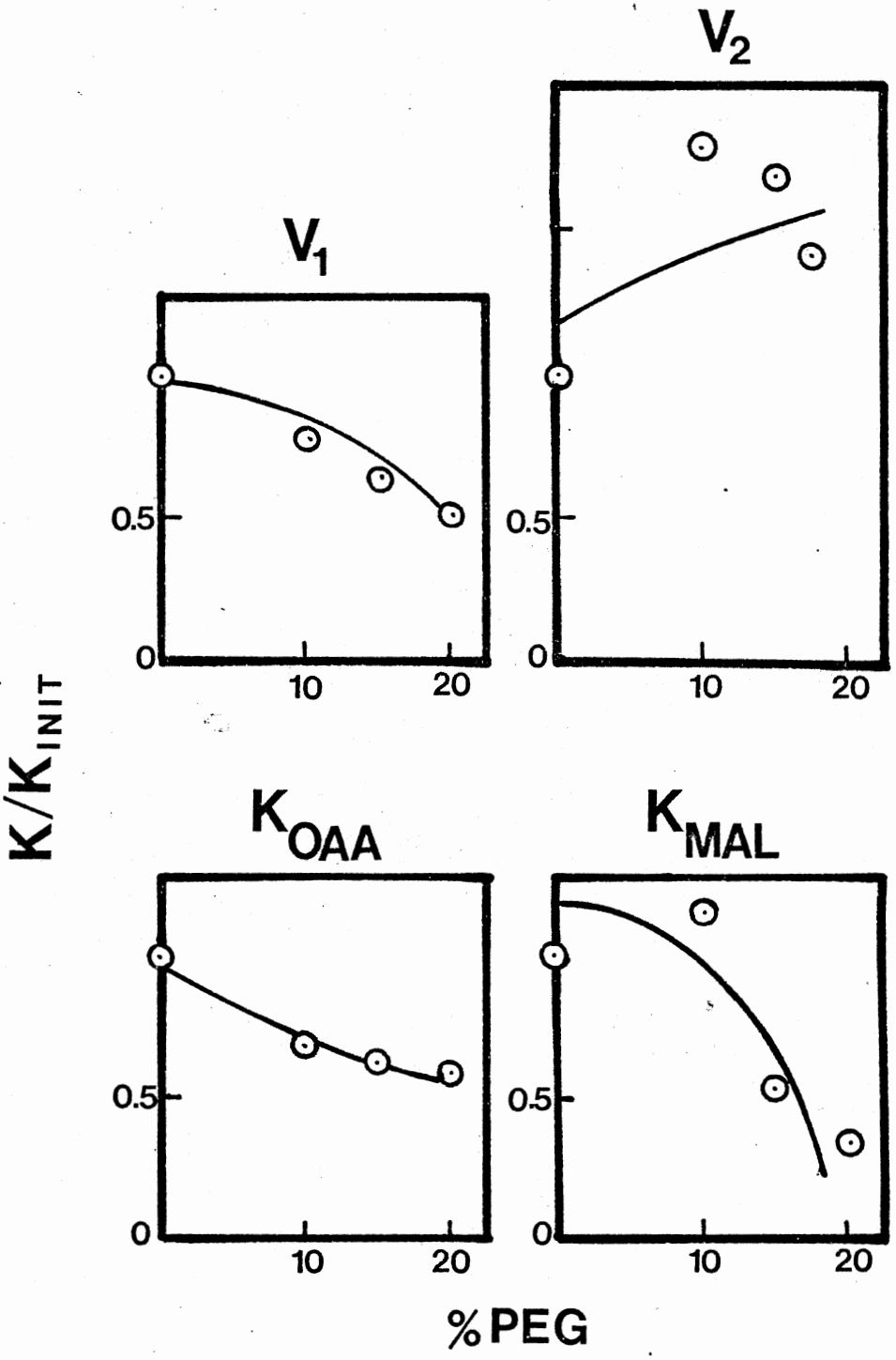
V2
V1
K/K INIT
0.5
0
10
20
KOAA
KMAL
%PEG

TABLE V

LAG TIMES OF THE MDH,CS COUPLED REACTIONS

Solution	Predicted Lag Time (sec)	Measured Lag Time (sec)
14% PEG	19	18[a]
No PEG	22	20[b]

[a]Mixture consisted of 0.26 µg/ml MDH, 0.144 µg/ml CS, 0.1 mM Acetyl CoA, 1 mM NAD, 2.5 mM Malate, 1 mM DTNB, 14% (w/v) PEG (6000), 10 mM potassium phosphate buffer, pH 7.5, at room temperature.

[b]Mixture consisted of 0.14 µg/ml MDH, 0.125 µg/ml CS, 0.1 mM Acetyl CoA, 1 mM NAD, 2.5 mM Malate, 2 mM DTMB, 10 mM potassium phosphate buffer, pH 7.5, at room temperature.

Palmitoyl-CoA Inhibition

Palmitoyl-CoA normally inhibits MDH. If GDH is added to the system, palmitoyl-CoA induces association between GDH and MDH, and palmitoyl-CoA binds to GDH rather than MDH in the complex. Thus, GDH protects MDH from palmitoyl-CoA inhibition (13). A 400-fold excess of CS to MDH, also, protected MDH from palmitoyl-CoA inhibition (10). On the basis of these experiments it seemed possible that palmitoyl-CoA could be inducing a weak attraction between MDH and CS which could be measured by a reversal of the palmitoyl-CoA inhibition of MDH. I tested whether 5% PEG could enhance this attraction to the point that a 3-fold excess of CS to MDH would prevent the palmitoyl-CoA inhibition. Figure 9 shows that the presence of CS raised the palmitoyl-CoA concentration required for 50% inhibition from 23 μM to 45 μM. However, this is reasonably explained by the fact that CS binds 15-20 mole of palmitoyl-CoA (50) per mole of enzyme and would reduce the effective palmitoyl-CoA concentration. The 3-fold excess CS does not have an effect that needs to be explained by heterologous association.

Isotope Incorporation Measurements

As discussed in the introduction, Bryce et al. (1) measured apparent anomalies in the coupled reactions catalyzed by aspartate aminotransferase and malate dehydrogenase (Equation 1-1a, 1-1b). They started these reactions with [^{14}C]Asp and a known amount of added unlabeled OAA. After a predetermined time, the reaction was terminated and the ratio of specific radioactivity of malate to that of aspartate,

Figure 9. Palmitoyl-CoA Inhibition of MDH in the Presence and Absence of CS. Solutions containing 5 mM potassium phosphate buffer, pH 7.5, 5% PEG (6000), 1 mM EDTA, 0.05 mg/ml MDH and/or 0.15 mg/ml CS were incubated overnight at 5°C with increasing concentrations of palmitoyl-CoA. (●), MDH specific activity in the presence of CS; (o), MDH specific activity in the absence of CS.

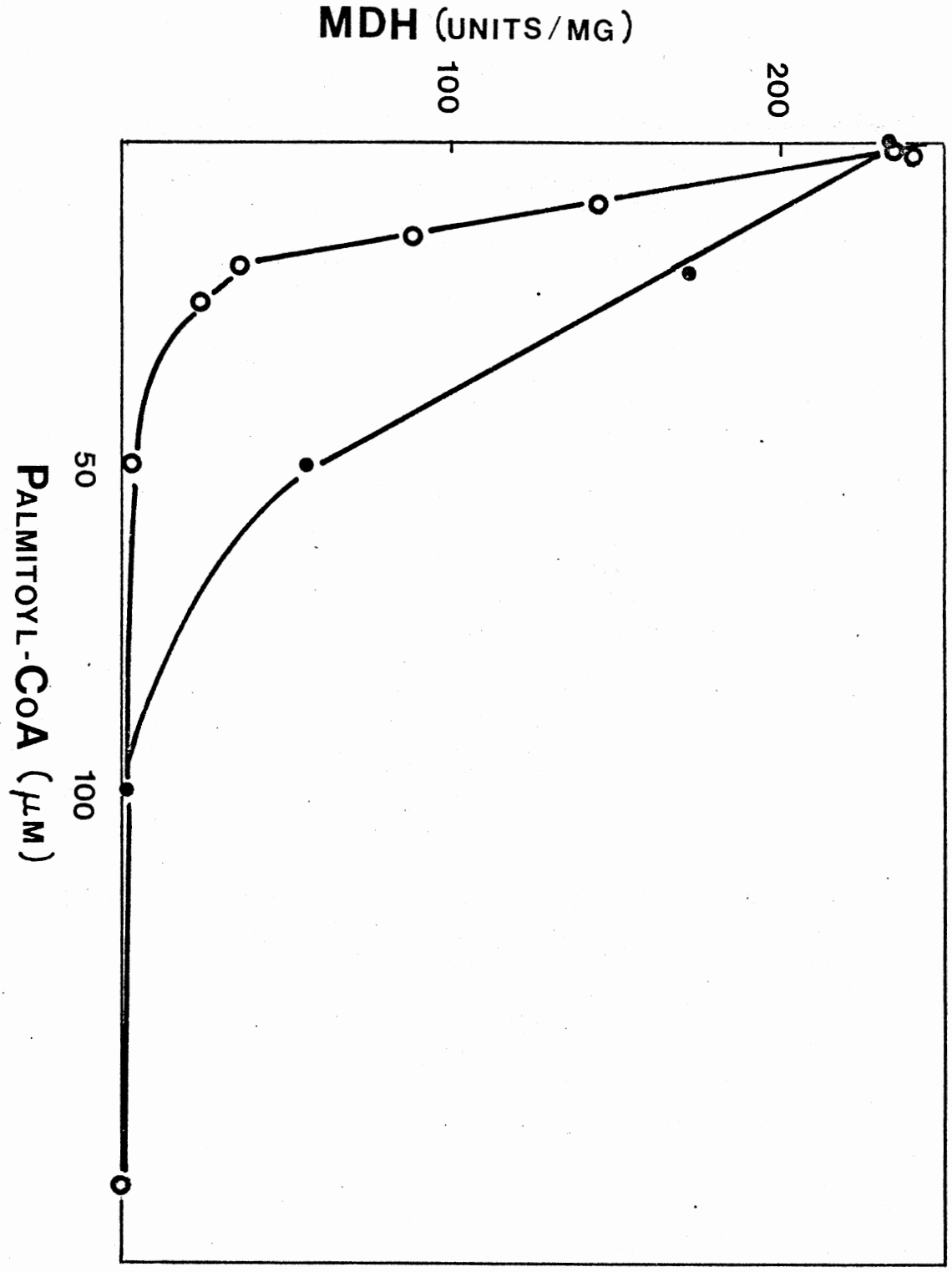
MDH (UNITS/MG)
100
200
50
100
PALMITOYL-COA (μM)

r, was measured. Under their conditions and with no anomalies, a significant amount of unlabelled Mal should have been produced from the unlabelled, exogenous OAA. This unlabelled Mal should have diluted the specific radioactivity of Mal produced by the coupled reaction from that of the [^{14}C]Asp, resulting in an r value of 0.16. Instead, they obtained an experimental value of r equal to 1.01 and 1.02 in two experiments and argued that this was evidence for the OAA isomer model. As will be discussed in Chapter IV, we believe this conclusion is invalid as a result of both logic errors in predicting consequences of the isomer model, and experimental errors in measuring the isotope ratios. The latter errors which result from massive decomposition of OAA catalyzed by the anion exchange resin are discussed next.

After quenching the coupled reactions (Equations 1-1a, 1-1b) and before measuring malate specific radioactivity, [^{14}C]Mal has to be separated from [^{14}C]OAA and [^{14}C]Asp. In Bryce's procedure (1) the quenched reaction mixture was first applied to a Dowex-50 cation exchange column on which the [^{14}C]Asp was retained. The radioactive eluate was then loaded on a Dowex-1 anion exchange column by which malate is widely resolved from the oxaloacetate by elution with a linear gradient of increasing HCl concentrations. When I attempted to repeat this experiment large quantities of radioimpurities were eluted over a broad elution volume including the malate peak (Figure 10). The resulting radioactivity per mole of malate was increased giving an impossibly high specific activity (r) of 3.8 for the isotope peak fraction (Peak C in Figure 10). When MDH was omitted from the reaction mixture, radioimpurities were still produced (Figure 11) which eliminates Mal as the source of the impurities. When both AAT and

Figure 10. Radioactivity Eluted from the Anion Exchange Column. The reaction mixture from the isotope incorporation experiment contained (at zero time after mixing) 37.5 μM NADH, 1.0 mM α-ketoglutarate, 8.0 μM oxaloacetate, 2.5 mM aspartate (0.85 Ci/mol), aminotransferase (v = 2.5 $\mu mol \cdot min^{-1} \cdot ml^{-1}$) and dehydrogenase (V = 4.3 $\mu mol \cdot min^{-1} \cdot ml^{-1}$). The enzymes and NADH in one stopped-flow drive syringe were mixed with the other reactants in syringe 2 and the reaction quenched with an equal volume of 0.44 M $HClO_4$ (0.22 M after mixing) in the third drive syringes. Reaction time was 0.10 s. Quenched reaction mixtures were collected and subjected to analysis as specified under "Isotope Indorporation, Experimental" involving cation and anion exchange chromatography. The radioactivity shown was eluted from the anion exchange column with a linear gradient made from 850 ml each of H_2O and 33 mM HCl.

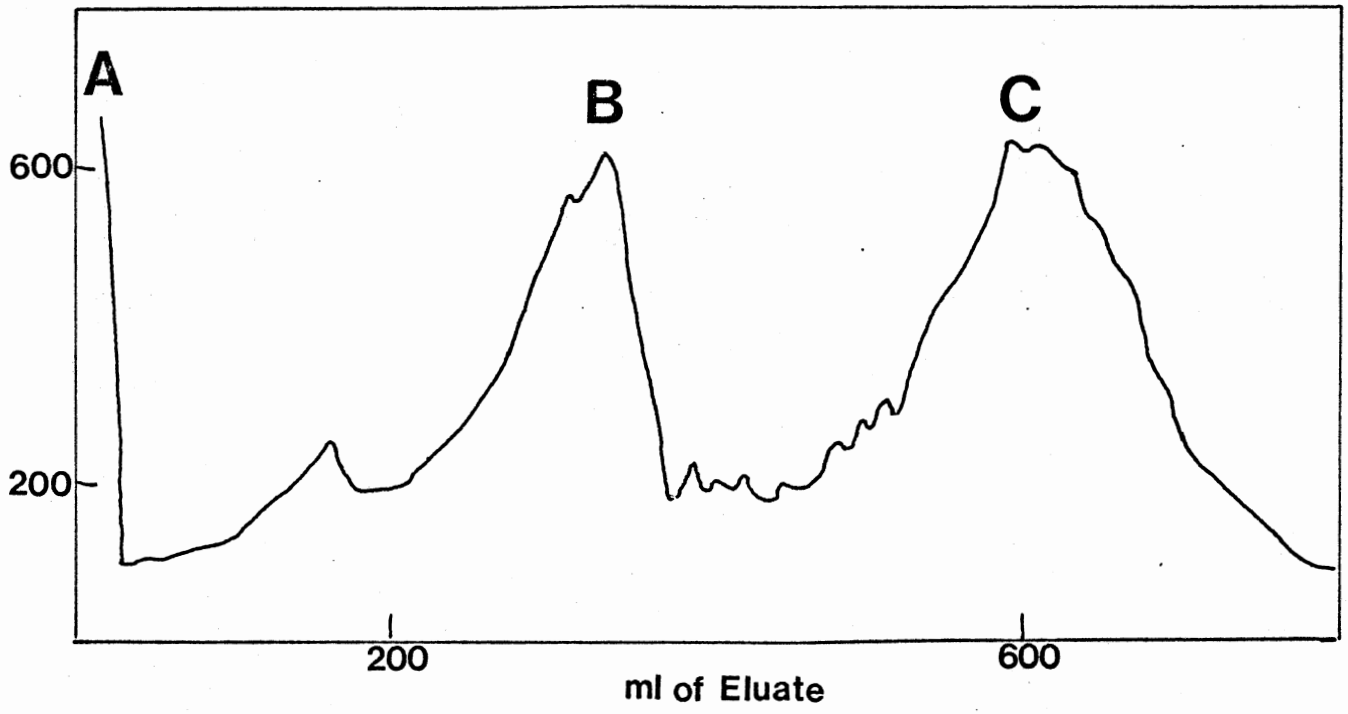
A
B
C
600
200
200
600
ml of Eluate

Figure 11. Radioactivity Eluted from Anion Exchange Column. The quenched reaction was carried out as described in the legend to Figure 10 except MDH was omitted and AAT concentration was 2.3 $\mu mol \cdot min^{-1} \cdot ml^{-1}$. The radioactivity shown was eluted from the anion exchange column with a linear gradient made from 850 ml each of H_2O and 33 mM HCl.

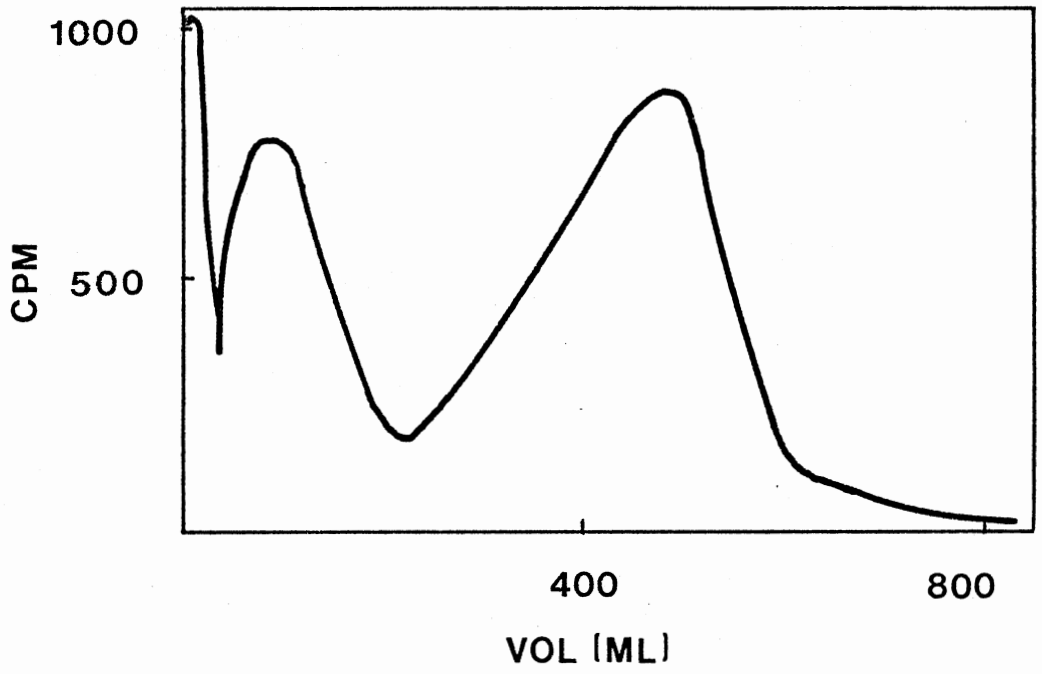
1000
500
CPM
400
800
VOL (ML)

MDH were omitted from the reaction, leaving [^{14}C]Asp as the only isotope, no radioimpurities were obtained. Thus [^{14}C]OAA must be the source of impurities. The radioactivity in Figure 10 and 11, however, must have arisen from decomposition products of OAA rather than OAA itself since OAA elutes near a 1300 ml elution volume.

We investigated where in the procedure OAA decomposed. From the acid concentrations involved, a pH of nearly 0.7 is calculated for the chemically quenched reaction mixture and pH values of: 1, and 2.4 to 1.8, are calculated for the cation and anion exchange chromatography solutions, respectively. Since oxaloacetate has been reported to be unstable below pH 3.0 (51), oxaloacetate might be expected to decompose during quenching and analysis of the reaction mixture. But, Figure 12 shows that little decomposition occurred within five hours at pH 0.7 which is longer than needed for chemical quenching and analysis. A remaining possibility is that oxaloacetate decomposition is catalyzed by the anion exchange resin to which it binds. This hypothesis was verified by loading a freshly prepared 45 mM OAA solution onto the same anion exchange resin used for analyzing the enzymatic reaction mixture. The solutes were eluted with a HCl gradient from 0 to 33 mM as before, but 17-fold steeper (100 ml total eluant). In spite of this much quicker than normal elution (within about 10 min), only about 0.3% of the OAA used was recovered by enzymatic assay. From this and replicate experiments we estimate that oxaloacetate decomposed more than 99% on the anion exchange resin.

The mechanism and products of this decomposition are not known. None of the products appear to be pyruvate which in a separate experiment was shown to elute in about 775 ml. Such a peak was not observed

Figure 12. OAA Decomposition in Solution. The concentration of OAA 2.2 mM initially) was measured enzymatically at various times after incubation in 0.22 M perchloric acid (o) or 100 mM Tris, pH 7.5 (●) at room temperature.

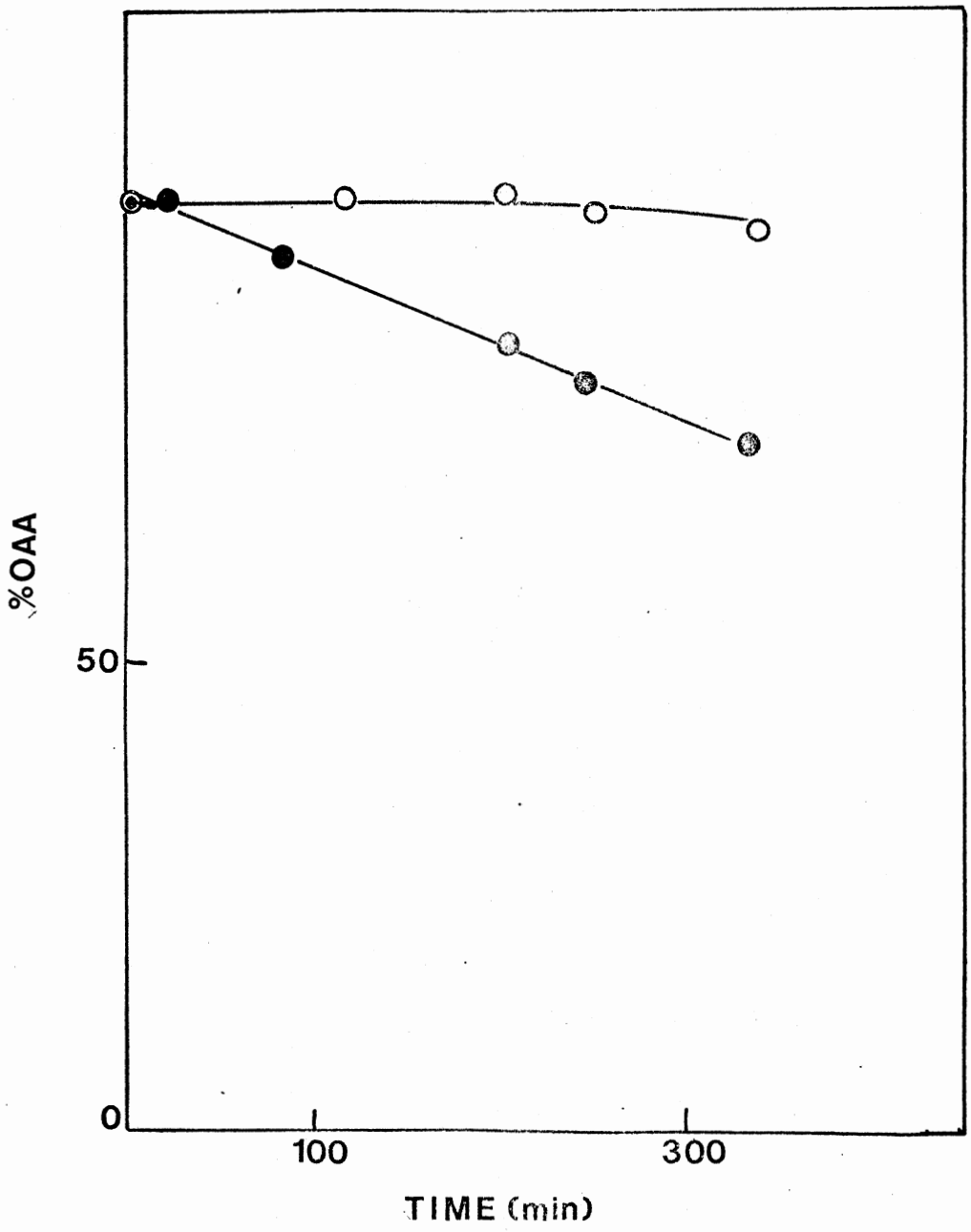
%OAA
50
0
100
300
TIME (min)

in Figure 10 and 11. To assess the effect of pH on this decomposition, OAA was also applied to this column in 10 mM Tris at pH 7.5 and the column washed for about 1½ hours with this buffer. A peak of oxaloacetate was then eluted with 5 M NaCl in the 10 mM Tris buffer (readjusted to pH 7.5); only 50% recovery of OAA was obtained. Unchromatographed OAA in the same buffer does not decompose over the same time period. These facts indicate that both anion exchange resin and protons catalyze decomposition of OAA. Proton catalysis alone is not adequate to cause significant errors in the isotope ratio measurements, however.

CHAPTER IV

SUMMARY AND CONCLUSIONS

Conclusions About Polymer Effects on MDH and CS

This study obtained information about the association behavior of a soluble MDH,CS mixture. As discussed in the Introduction, the precipitated enzymes are associated into a heterologous complex, which opens the question, "What portion of the soluble MDH,CS mixture exists in this complex?" In this section I will discuss the results that addressed this question, propose a model explaining the data, and propose additional experiments to answer remaining questions.

The general effect of increasing PEG concentrations is to cause increasing extents of enzyme polymerization either in the mixture or of each enzyme alone. Increasing PEG molecular weight causes a disproportionate increase in the extent of polymerization (Figure 4). As discussed in the Introduction, the same PEG molecular features which cause phase separations probably also induce the formation of the large soluble enzyme complexes.

Sedimentation velocity measurements were made to ascertain whether the complexes contain a major fraction of the total enzymes (Table III). We attempted to detect PEG induced association in the following system: 1 mg/ml MDH, 1 mg/ml CS, 5 mM potassium phosphate buffer, pH 7.5, at 5°C with 0, 20 and 100 μM palmitoyl-CoA. 10% PEG precipitates the

system with no palmitoyl-CoA and the majority of the enzyme was found unassociated in 5% PEG (Table III). Why doesn't extensive asscoiation occur in this system? 1) Possibly, near precipitating PEG concentrations are required to force a majority of enzyme to polymerize. 2) Recent results indicate that decreasing the pH from 7.5 to 7.0 and raising the temperature from 5°C to 10°C dramatically decreases the solubility of the MDH,CS mixture relative to MDH alone. pH 7.0 and 10°C were the conditions of Halper and Srere's experiments (11) in which they detected formation of the precipitated heterologoux complex. Possibly, our slight alteration of conditions resulted in a system in which a major amount of the precipitated heterologous complexes and, therefore, a major amount of soluble heterologous complexes do not form.

6% PEG precipitates the system consisting of 1 mg/ml MDH, 1 mg/ml CS, 5 mM potassium phosphate pH 7.5, and 20 μM palmitoyl-CoA at 5°C. The sedimentation velocity measurements (Table III) indicate that the majority of enzyme is unassociated at the near precipitating PEG concentration of 4%. This measurement is somewhat uncertain due to problems with instability at the synthetic boundary. 20 μM palmitoyl-CoA was stoichiometric with the enzymes. Raising the palmitoyl-CoA concentration to 100 μM caused the majority of enzymes to polymerize in 1% PEG (Table III). We do not know yet whether this occurs in the absence of PEG, and whether association is homologous or heterologous. In summary: 1) if enzyme complexes in the absence of palmitoyl-CoA ever contain a major fraction of the total enzyme, the conditions under which this occurs are very selective; 2) excess palmitoyl-CoA appears to induce polymerization of the majority of enzyme in an MDH,CS,PEG system.

We attempted to ascertain whether the complexes consisted of primarily self-associated (homologous) or cross-associated (heterologous) enzymes. The following tests required examining complexes formed in the system: 27.5 μg/ml MDH, 27.5 μg/ml CS, 27.5 mM potassium phosphate buffer, pH 7.5 at room temperature and varying PEG concentrations. In this system precipitated heterologous complexes apparently form because 25% PEG causes the mixture of MDH and CS to become slightly turbid, while each enzyme alone remains soluble (Table II). However, the following data suggest the complexes are primarily homologous below the precipitating, (25%) PEG concentrations. 1) The complexes in 1% PEG are primarily homologous (Figure 5). 2) No more of each enzyme was associated in the enzyme mixture plus 0, 10, 15 and 20% PEG than in the separate solutions plus each PEG concentration (Figure 3). For this to have occurred with a conversion from primarily homologous to primarily heterologous complexation would require a coincidental and unlikely set of equilibria. 3) The kinetics of MDH in 0, 10, 15, and 20% PEG were measured in the presence and absence of CS (Figure 7 and Figure 8). Addition of CS did not seem to alter MDH kinetics. This indicates (but does not prove) that little heterologous association had occurred.

If little heterologous association occurs in the solution phase the precipitation process itself must induce the extensive heterologous association. This may be at first surprising. However, further consideration shows that a large amount of the precipitated heterologous complex has to form regardless of its equilibrium prior to precipitation. As discussed in the Introduction, PEG can precipitate the mixture of MDH and CS while each enzyme alone is soluble. The only reasonable

explanation is that a heterologous complex forms which is less soluble than either enzyme alone. Therefore, a sufficient PEG concentration will precipitate the heterologous complex while leaving the homologous and unassociated protein in solution. Removal of the heterologous complexes from the solution phase equilibrium by precipitation will shift the reaction towards extensive heterologous association.

A large extent of MDH-CS association in the soluble mixture may not occur. However, the specific interaction between these two enzymes, adjacent to each other in their metabolic pathways, makes one wonder if it could occur without a physiological basis. One speculation is that these two enzymes exist in the mitochondrial matrix as the precipitated heterologous complex. This is not unreasonable. A recent report by Srere (52) presents evidence that the total protein concentration of the rat-liver mitochondrial matrix is over 50% by weight, and enzymes probably exist and behave as a multienzyme complex rather than as enzymes in solution. Citrate synthase and malate dehydrogenase, when immobilized as a multienzyme system, would have an advantage over enzymes in free solution. Their intermediate substrate, OAA, could be passed directly from the active site of the first enzyme, which produced it, to the active site of the second enzyme for utilization.

A variety of measurements in this thesis required changing conditions from those in which Halper and Srere characterized heterologous association. It is possible that the shifted conditions (temperature, enzyme concentration, buffer concentration, pH and incubation time may all be important) abolished heterologous association. A set of measurements should be made under conditions in which formation of the precipitated heterologous complex has been clearly demonstrated, and

which are as similar as possible to those of Halper and Srere's. The system I would test is: 5 mM potassium phosphate buffer, pH 7.0, 1 mg/ml MDH, 1 mg/ml CS, at 10°C after 1 hour of incubation. So, before ruling out the possibility of extensive PEG-induced heterologous association of soluble MDH and CS the following tests should be made. 1) The effect of increasing PEG concentration on the solubility of the mixture of enzymes should be compared to the solubility of each enzyme alone. A lowered solubility of the enzyme mixture will demonstrate formation of the precipitated heterologous enzyme complex. 2) Sedimentation velocity measurements should be made in the same system used in test 1, plus near precipitating PEG concentrations. This will rule out or prove that extensive association can occur in the solution phase. 3) Dynamic light scattering measurements should be made in the same solutions used in test 2. DLS will establish the existence and size of polymerized enzyme, even if it contains only a small fraction of total enzyme. 4) It may be possible to characterize the composition of the complexes formed in the solutions used with test 2 and 3 using the method described in Figure 5 and the following modifications. After addition of DTP to the 10°C solution the reaction should be allowed 15 hours (at 10°C) to go to completion. Since 5 mM potassium phosphate is not sufficient to maintain a constant pH, DTP will have to be added in small amounts adjusting the pH back to 7.0 after each addition.

Besides these experiments to further clarify the system of MDH, and CS alone in PEG, information about polymer effects on MDH and CS under other conditions would be important. We found that 100 μM palmitoyl-CoA caused extensive enzyme association with 1 mg/ml MDH, 1 mg/ml CS, and 1% PEG (Table III). Is this association heterologous? What are the kinetic

consequences of this association? Are the properties of palmitoyl-CoA inhibition changed? Other important questions are: 1) What is the effect of lipid binding on PEG induced association? Some data indicate that MDH may exist in vivo as a lipid bound protein (see Introduction). This could change its association properties by causing conformational changes or by allowing binding directly through the lipid. 2) Do other more physiological polymers such as dextran, nucleic acids, or other types of protein have the same effect as PEG? 3) What are the catalytic properties of the MDH-CS heterologous complex which exists in the precipitated form?

Isotope Incorporation Experiment

In this section I will discuss the isotope incorporation experiment of Bryce et al. (1) in terms of possible molecular explanations and in light of the results from this thesis. Bryce's results indicated that the labelled malate produced by the coupled reaction was undiluted by unlabelled malate, produced from external OAA. As Bryce et al. stated, the only way this could have occurred is, "If the labelled oxaloacetate reaches the malate before equilibration with the unlabelled oxaloacetate and binding of the unlabelled oxaloacetate is also effectively prevented ..." To explain this, they proposed that the aminotransferases produce an active OAA isomer (different from either the keto or enol forms), which reaches the dehydrogenase in a few microseconds before conversion to its predominate and less active form in solution. The external OAA exists primarily in the less active form. However, the hypothesis " ... binding of the unlabelled oxaloacetate is also effectively prevented ... " cannot be achieved unless an AAT-MDH

complex forms which saturates the dehydrogenase with enzymatically produced oxaloacetate or sterically blocks access of exogenous OAA to the MDH active sites. What Bryce et al. may have meant was that the binding and hence the use of unlabelled OAA was negligible with respect to use of enzymatically produced (labeled) OAA. This overlooks the fact that proposing an increase in reactivity of labelled OAA causes its concentration in the coupled reactions to decrease. Therefore, the concentration of the reactive form of the exogenous OAA is never negligible relative to that of the enzymatically produced OAA. Calculations and explicit equations (2) reveal that the existence of a more active OAA isomer could raise the expected r value from 0.16 to a maximum of 0.53, but not to the value of 1 that they measured. The only molecular models which can reasonably explain an r value of 1 requires the existence of an MDH-AAT complex. However, no association was observed in their experiments that they ran to detect complex formation. Therefore, it seems extremely unlikely that undiluted, radioactive malate was actually produced under these conditions.

Instead, the results in this thesis indicate that contamination by radioactive OAA decomposition products raised the measured malate specific radioactivity value artificially. These radioimpurities eluted throughout the region that malate elutes and were never cleanly resolved. Would there be enough OAA in the quenched reaction mixture to cause the errors claimed? To judge this we calculated the quantities of [^{14}C]OAA, and [^{14}C]Mal, which came from the pool of [^{14}C]Asp and were present at the quench time of the reactions (2). Calculated results are 1.7 μM [^{14}C]OAA, 0.078 μM [^{14}C]Mal and r = 0.097 for experiment 1 of Bryce et al. (1) and 3.3 μM [^{14}C]OAA, 0.90 μM [^{14}C]Mal, and r = 0.22

for our experiments. To observe an r of 1.0 as they did would require that radioactivity from oxaloacetate decomposition be about 10 times as much from the malate assayed. This is reasonable, considering decomposition products from the 20-fold excess of [^{14}C]OAA to [^{14}C]Mal would mask the [^{14}C]Mal elution peak position. We measured a specific activity ratio of 3.8 (experiment described in Figure 10 legend); this is also reasonable since our assays of malate were made on the major fractions of peak C in Figure 10, which was predominantly an impurity. So in view of the calculated excess of [^{14}C]OAA to [^{14}C]Mal, the massive decomposition of OAA on the anion exchange columns and the lack of resolution of these products from malate, this method would be expected to give unreliable measures of the malate specific radioactivity.

The decomposition of OAA on anion exchange columns could be important in experiments for other objectives. In particular, it may be wise to test more carefully for oxaloacetate decomposition in procedures for measuring oxaloacetate levels in tissue. There are enormous differences in published values for the cellular concentration of this important metabolite (28, 53, 54). Although none of the four procedures used for measurement of cellular oxaloacetate concentration utilize anion exchange chromatography, it is conceivable that soluble cations in tissue extracts bind oxaloacetate and accelerate its decomposition.

Use of Dynamic Light Scattering

Dynamic light scattering (DLS) data have given clear evidence of large enzyme complexes. These data are easy to gather and are direct in that they do not require chemical or physical alterations of the system.

Potentially the DLS data can also reveal the distribution of molecular sizes and the weight fraction of enzyme in the complexes. The unusually large size of these enzyme complexes and their heterogeneity in size complicates these calculations, however, and it remains to be seen whether the complications can be overcome. The large molecular sizes cause destructive interference of scattered light. The correction factors for this effect F (called form factors) are a function of particle size, shape, and the scattering angle θ. We assume the shapes are spherical based on our electron microscope data and we know θ. The dependence on size, however, makes the solution for F dependent on the solution for a size distribution function ω (solution of the heterogeneity problem). That is both F and ω appear in the model equation and neither can be independently determined.

Three computer methods exist which can in principle solve the above equations with appropriate DLS data. These are the methods of cumulants (34), histogram (35), and simulation, but they have practical limitations the extents of which are not yet clear with the latter two methods. Our particle size distribution is probably too broad to permit use of the cumulant method and the histogram method has not, to our knowledge, been applied to as demanding a task as we have. The simulation method appears very promising to us. With this technique, one assumes a distribution function from which precise DLS can be generated ("simulated"), including the correction factors F. The adequacy of the distribution function is judged by comparison of the simulated with real DLS data. Since for large particles, F depends on θ and size so sensitively, and data can be obtained over a large range of angles, the simulation method may establish a reasonable unique distri-

bution function. Even if only a range of possible distribution functions is determined, the insights gained from these calculations will quite likely be valuable in guiding other experimental and analysis work.

A SELECTED BIBLIOGRAPHY

(1) Bryce, C. F. A., Williams, D. C., and John, R. A. (1976) Biochem. J. 153, 571-577.

(2) Manley, E. R., Webster, T. A., and Spivey, H. O. (1980) Arch. Biochem. Biophys., in press.

(3) Albertsson, P. (1971) Partition of Cell Particles and Macromolecules, Wiley-Interscience, New York.

(4) Bailey, F. E., and Koleske, J. V. (1976) Poly(ethylene oxide), Academic Press, New York.

(5) Miekka, S. I., and Ingham, K. C. (1978) Arch. Biochem. Biophys., 191, 525-536.

(6) Herzog, W., and Weber, K. (1978) Eur. J. Biochem., 91, 249-254.

(7) Fenton, J. W., II, and Fusco, M. J. (1974) Thrombosis Res., 4, 809.

(8) Rumpling, M. W., Lane, D. A., and Kakkar, V. V. (1976) Thrombosis Res., 9, 379-386.

(9) Bachman, L., and Johansson, G. (1976) FEBS Letters, 65, 39-43.

(10) Fahien, L. A., and Kmiotek, E. (1979) J. Biol. Chem., 254, 5983-5990.

(11) Halper, L. A., and Srere, P. A. (1977) Arch. Biochem. Biophys., 184, 529-534.

(12) Fahien, L. A., and Smith, S. E. (1974) J. Biol. Chem., 249, 2696-2703.

(13) Fahien, L. A., and Kmiotek, E., and Smith, L. (1979) Arch. Biochem. Biophys., 192, 33-46.

(14) Yoshida, A. (1966) J. Biol. Chem., 241, 4966-4976.

(15) Hulme, E. C., and Tipton, K. F. (1971) FEBS Lett., 12, 197-200.

(16) Hill, D. E., and Hummes, G. G. (1975) Biochemistry, 14, 203-213.

(17) Frieden, C., and Colman, R. F. (1967) J. Biol. Chem., 242, 1705-1715.

(18) Uyeda, K., and Luby, L. J. (1979) J. Biol. Chem., 249, 4562-4570.

(19) Weber, G. (1972) Biochemistry, 11, 864-878.

(20) Banaszak, L. J., and Bradshaw, R. A. (1975) The Enzymes, Vol. 2, P. B. Boyer, ed., Academic Press, New York, 369-396.

(21) Thorne, C. J. R., and Kaplan, N. O. (1963) J. Biol. Chem., 238, 1861-1868.

(22) Kaun, K. E., Jones, G. L., and Vestling, C. S. (1979) Biochemistry, 18, 4366-4373.

(23) Dodd, G. H. (1973) Eur. J. Biochem., 33, 418-427.

(24) Webster, K. A., Patel, H. V., Freeman, K. B., and Papahadjopoulous, D. (1979) Biochem. J., 178, 147-158.

(25) Jones, G. L., and Vestling, C. S. (1978) Federation Proc., 37, Abst. 2799.

(26) Kawaguchi, A., and Bloch, K. (1975) J. Biol. Chem., 249, 5793-5806.

(27) Kawaguchi, A., and Bloch, K. (1977) J. Biol. Chem., 251, 1406-1412.

(28) Siess, E. A., Brocks, D. G., Lattke, H. K., and Wieland, D. H. (1977) Biochem. J., 166, 225-235.

(29) Spector, L. B. (1972) The Enzymes, Vol. 7, P. B. Boyer, ed., Academic Press, New York, 357-368.

(30) Bergmeyer, H. U., Bernt, E., Mollenng, H., and Pfleiderer, G. (1974) Methods of Enzymatic Analysis, Vol. 4, H. U. Bergmeyer, ed., Academic Press, New York, 1696-1700.

(31) Mollenng, H. (1974) Methods of Enzymatic Analysis, Vol. 3, H. U. Bergmeyer, ed., Academic Press, New York, 1589-1599.

(32) Beme, B. J., and Pecora, R. (1976) Dynamic Light Scattering, John Wiley and Sons, Inc., London.

(33) Cohen, R. J. and Benedek, G. B. (1976) J. Mol. Biol., 108, 151-178.

(34) Koppel, D. E. (1972) J. Chem. Phys., 57, 11-19.

(35) Gulari, E., Gulari, E., Tsunashima, Y., and Chu, B. (1974) J. Chem. Phys., 70, 3965-3972.

(36) Cay, B. (19) "Laser Light Scattering".

(37) McGurk, K. S. (1976) Ph.D. Thesis, Oklahoma State University.

(38) Lindberg, M. and Mosback, K. (1975) Eur. J. Biochem., 53, 481-486.

(39) Pharmacia Fine Chemicals (1977) Affinity Chromatography, Principles and Methods, Rahms i Lund, Sweden, 10.

(40) Chervenka, C. H. (1970) A Manual of Methods for the Analytical Ultracentrifuge, Spinco Division of Beckman, Inc., Palo Alto, California.

(41) Chandler, J. P., Hill, D. E., and Spivey, H. O. (1972) Comput. Biomed. Res., 5, 515-534.

(42) Mclure, W. R. (1969) Biochemistry, 8, 2782-2786.

(43) Hummel, J. P. (1949) J. Biol. Chem., 180, 1225-1228.

(44) Webster, T. A., Merz, J. M., Appleman, J. R., Ackerson, B. J., Spivey, H. O., and Manley, E. R. (1980) American Society of Biological Chemists, 71st Annual Meeting, Abst. #153.

(45) Manley, E. R., Webster, T. A., Appleman, J. R., Ackerson, B. J., and Spivey, H. O. (1979) 22nd West Central States Biochemical Conference.

(46) Hunter, M. J. and Ludwig, M. L. (1962) J. Am. Chem. Soc., 84, 3491-3504.

(47) Atha, P. H., and Ingham, K. C. (1980) American Society of Biological Chemists 71st Annual Meeting, Abst. 3183.

(48) North, F. C. (1977) Ph.D. Thesis, Oklahoma State University.

(49) Schumaker, V. N., and Shachman, H. K. (1957) Biochim. Biophys. Acta, 73, 628-639.

(50) Srere, P. A. (1965) Biochim. Biophys. Acta, 106, 445-455.

(51) Wahlefeld, A. W. (1974) Methods of Enzymatic Analysis, Vol. 3, H. U. Bergmeyer, ed., Academic Press, New York, 1607.

(52) Srere, P. A. (1980) TIBS, 5, 120-121.

(53) Srere, P. A. (1976) Gluconeogenesis, Its Regulation in Mammalian Species, R. W. Hanson and M. A. Mehlman, eds., John Wiley, New York, 158.

(54) Tischler, M. E., Friedrichs, D., Coll, K., and Williamson, J. R. (1977) Arch. Biochem. Biophys., 184, 222-236.

PART TWO

PROTON AND MAGNESIUM BINDING TO 5-PHOSPHORIBOSYL α-1-PYROPHOSPHATE

CHAPTER I

INTRODUCTION

5-Phosphoribosyl α-1-pyrophosphate (PRPP) is an important substrate for purine, pyrimidine and NAD^+ biosynthesis as it is the source of the D-ribose-5-phosphate moiety in salvage pathways and in de novo synthesis (1, 2).

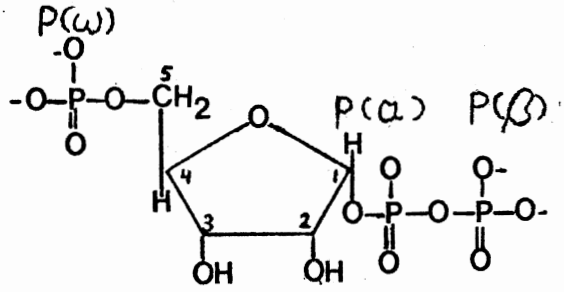

PRPP

In pyrimidine synthesis, orotate phosphoribosyltransferase attaches orotic acid to the 5-phosphoribosyl moiety of PRPP yielding orotidine 5'phosphate:

$$\text{Orotic acid} + \text{PRPP} \xrightarrow{\text{orotate phosphoribosyltransferase}} \text{Orotidine 5'-phosphate} + PP_i \qquad (1)$$

In purine synthesis PRPP reacts with glutamine so that the amino group from the amide portion of glutamine displaces the pyrophosphate group from the 1 position in PRPP yielding 5-phospho-β-D-ribosylamine:

$$PRPP + Gln \xrightarrow{\text{glutamine amidophosphoribosyltransferase}} Glu + PP_i + \text{5-Phospho-}\beta\text{-D ribosylamine} \quad (2)$$

Free purines formed from nucleotides are salvaged in vertebrates for reuse in nucleotide and nucleic acid biosynthesis. The major mechanism is by action of adenine phosphoribosyltransferase and guanine (or hypoxanthine) phosphoribosyltransferase, which attach the purine to the D-ribose-5-phosphate moiety of PRPP as follows:

$$\begin{aligned} \text{Adenine} + PRPP &\rightleftharpoons AMP + PP_i \\ \text{Guanine} + PRPP &\rightleftharpoons GMP + PP_i \end{aligned} \quad (3)$$

PRPP is a substrate for NAD^+ synthesis (2). In the presence of a single enzyme from liver, quinolinic acid is condensed with PRPP, yielding quinolinic acid ribonucleotide, which is decarboxylated, producing nicotinic acid ribonucleotide. The latter is a precursor for NAD^+ synthesis, which is accomplished following condensation with ATP and amination with glutamine.

Mg^{2+} is required in many of these reactions and may reflect the use of Mg^{2+}-PRPP as the true substrate. Mg^{2+} activates AMP and GMP synthesis in the adenine and guanine phosphoribosyltransferase catalyzed reactions (Equation 3). The kinetics of this activation combined with the dissociation constant of MG_2PRPP indicates that this stimulation is increased by magnesium binding to PRPP (3). Human glutamine amidophosphoribosyl transferase (3) has an absolute requirement for a divalent cation, with the order of relative effectiveness being $Mg^{2+} = Mn^{2+} > Co^{2+} > Ca^{2+}$ (3). The enzyme which synthesizes PRPP, PRPP synthetase, requires $MgATP^{3-}$ as a substrate (4).

If MgPRPP, rather than PRPP is the substrate for PRPP synthesizing and utilizing enzymes, the stability constant of the MgPRPP must be known to properly design and interpret kinetic studies of these enzymes (5). For this reason Mg^{2+}- and H^{+}-PRPP stability constants were determined in our laboratory in a previous study utilizing the pH titration method (6). This method depends on the fact that Mg^{2+} and proton complexation to PRPP are coupled equilibria. Thus, variations in total Mg^{2+} concentrations will alter the "conditional proton stability constatns" (7) and vice versa. These alterations can be predicted by the various step stability constants and the equilibrium model scheme assumed. We assumed a model in which Mg^{2+} bound to the C-1-pyrophosphate groups (bidentate complex with hydroxyl ions of α and β phosphates) and also bound with lower affinity to the C-5-phosphate group of PRPP (monodentate complex). This assumption was strengthened by the resulting Mg^{2+}-PRPP stability constants calculated from the titration data. The first and second step stability constants for PRPP were in excellent agreement with those of MgADP and MgAMP, respectively (6).

Two questions from the above study deserved further investigation, however. First, were the model MgPRPP structures valid or could the similarity of results with MgADP and MgAMP be fortuitous and consistent with different MgPRPP and Mg_2PRPP structures? Secondly, the proton dissociation constant for Mg•H•PRPP was 1.0 pK unit below that of published values for Mg•H•ADP (8). Possible explanations for this difference in pK_a between Mg•H•PRPP and Mg•H•ADP are: a) the PP group on PRPP is attached to an anomeric carbon with different electron density than the C-(5)-PP of ADP, and b) the presumed Mg•H•PRPP

structures are incorrect.

The present NMR studies were planned to answer these questions. In principle, both structures and stability constants can be determined from NMR data. NMR determination of the Mg^{2+} stability constant of $MgPRPP^{3-}$ by Mg^{2+} titration of PRPP are not practical, however, due to the low PRPP concentrations needed before significant deviations from stoichiometric binding of Mg^{2+} to PRPP occur. These low PRPP concentrations are below the sensitivity of NMR measurements with practical data collection times. The NMR studies described here, therefore, were designed to elucidate the structure(s) of MgPRPP complex(es) and the H^{+} stability constants of MgPRPP and Mg^{2+} free-PRPP.

In this investigation possible structures of MgPRPP were examined with a space-filling molecular model of PRPP. This modelling demonstrated that bond angles and lengths allow Mg^{2+} to actually bridge the ribose ring and simultaneously bind phosphates on both sides. Figure 1 shows that Mg^{2+} can chelate the 1-pyrophosphate group (structure A) and it can also bind the P(ω) group on one side of the ring plus either the P(β), P(α), or C(1)-PP on the other side (structures B, C, and D, respectively). I attempted to elucidate which is the major structure.

The approach to this problem was to examine perturbations of the ^{13}C and ^{31}P NMR spectra caused by Mg^{2+} binding. Effects of proton and Mg^{2+} binding to phosphates on ^{31}P resonances have been reported in Cohn's study of Mg^{2+} binding to ADP and ATP (9). Protonation causes an upfield shift in the ^{31}P resonances of all known phosphate groups and this shift, caused by binding of the last dissociating proton to the ADP pyrophosphate group, is on the order of 60 Hz. Mg^{2+} binding to the ADP and ATP phosphates causes downfield shifts. At a pH of seven

Figure 1. Possible MgPRPP Structures. These structures were constructed with a space-filling molecular model of PRPP.

A

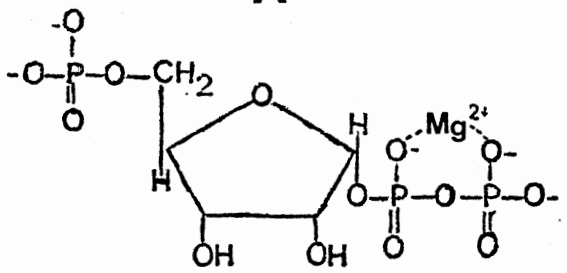

B

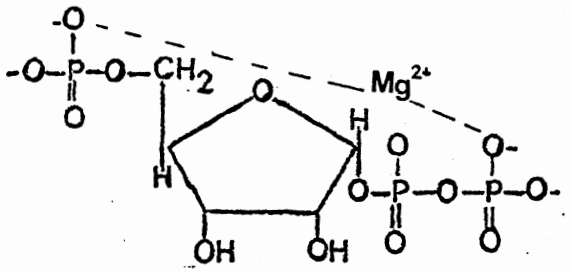

C

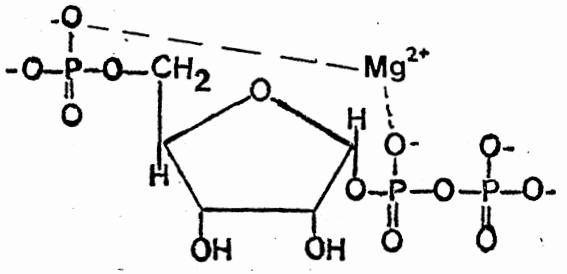

D

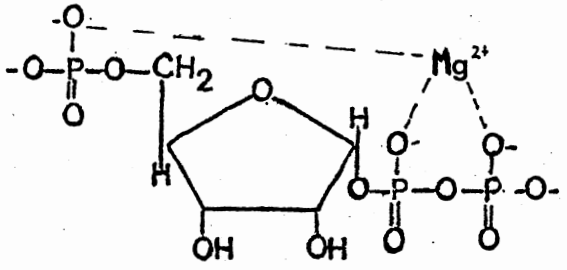

Mg^{2+} binding to ATP causes a downfield shift in the gamma and beta phosphorous signals of 1.7 and 26 ppm respectively, while little shift (0.20 ppm) is measured in the alpha phosphate signal, indicating predominant chelation to the beta and gamma phosphates. Mg^{2+} chelation to the ADP pyrophosphate causes downfield shifts in the C(5)-αP and C(5)-βP signals of 0.40 and 0.60 ppm, respectively. Proton and Mg^{2+} binding, therefore, causes easily measurable shifts.

CHAPTER II

EXPERIMENTAL PROCEDURE

Materials

The PRPP (Na^+ salt) and deuterium oxide were obtained from Sigma Chemical Co. The PRPP was considered to be between 80% and 90% pure based on 1) data supplied by Sigma, 2) or analyses of PRPP used in a previous study (6), and 3) its ^{31}P NMR spectra. The chemical analyses found the following impurities (6): 2.2% ribose-5-phosphate, 7.6% pyrophosphate, 12% ribose 1-5 diphosphate, and 2% phosphate. The NMR analyses involved comparing the area of the small impurity peaks to the PRPP peaks. To test whether major decomposition of a PRPP sample could occur during the 40 minute interim of an NMR measurement, one sample was pulsed overnight (temperature approximately 30°C). The impurity peak areas were initially 10.8% of the total, incubation overnight in the NMR instrument raised this to only 13.7%. Sigma reported a 99.8% purity of D_2O. Heavy metal contaminants were extracted from commercial $MgCl_2$ with dithizone (10) and the $MgCl_2$ recrystallized thereafter.

Methods

The NMR spectra were obtained with a Varian XL-100 NMR spectrometer operating at 40.3 MHz for ^{31}P resonance, and at 25.2 MHz for ^{13}C

resonance. Sample volumes were 2.5 ml in sample tubes of 12-mm outer diameter. The solvent water contained at least 10% D_2O for the purpose of providing a field frequency lock on the deuterium resonance. The ^{13}C and ^{31}P spectra were obtained in the Fourier transform mode and signal averaging was performed by a Nicolet TT 100 computer dedicated to the spectrometer. ^{31}P chemical shifts are expressed with respect to H_3PO_4 as an external reference. ^{13}C spectra were expressed with respect to TMS as an external reference.

Titration Curve

The PRPP was dissolved with or without equimolar $MgCl_2$ to make a solution of 0.1 M PRPP in either 10% D_2O or 100% D_2O. Small aliquots of HCl in H_2O were added to change the pH; these additions diluted the PRPP concentration by no more than 10%. For solutions with greater than 90% D_2O the pD was calculated from the pH meter reading by the following (11):

$$pD = pH + 0.40$$

As shown in Figure 2, the chemical shifts caused by the small dilution of PRPP, and changes of ionic strength caused by addition of titrant were negligible relative to the shifts (2-5 ppm) produced by the pH changes. Changing the H_2O concentration from pure H_2O to 10% D_2O did not change the pH meter reading.

It is possible that at low pH some of the equimolar Mg^{2+} may be displaced from PRPP (because of the coupled equilibrium between proton and Mg^{2+} binding). A great excess of Mg^{2+} would assure 100% Mg^{2+} bound PRPP. However since the purpose of this study was to study the

Figure 2. Control Experiments for PRPP Titrations

A) ^{31}P chemical shifts versus dilutions of an 0.1 M PRPP plus 0.1 M $MgCl_2$ solution in D_2O.

B) ^{31}P chemical shifts of 0.1 M PRPP in D_2O, pD 7.4, versus change of ionic strength. Ionic strength was increased by additions of NaCl.

C) ^{31}P chemical shifts of $^{31}P(\beta)$ in solution of 0.1 M PRPP plus (●-●) 0.125 M $MgCl_2$ or (o-o) 0.1 M $MgCl_2$ in D_2O.

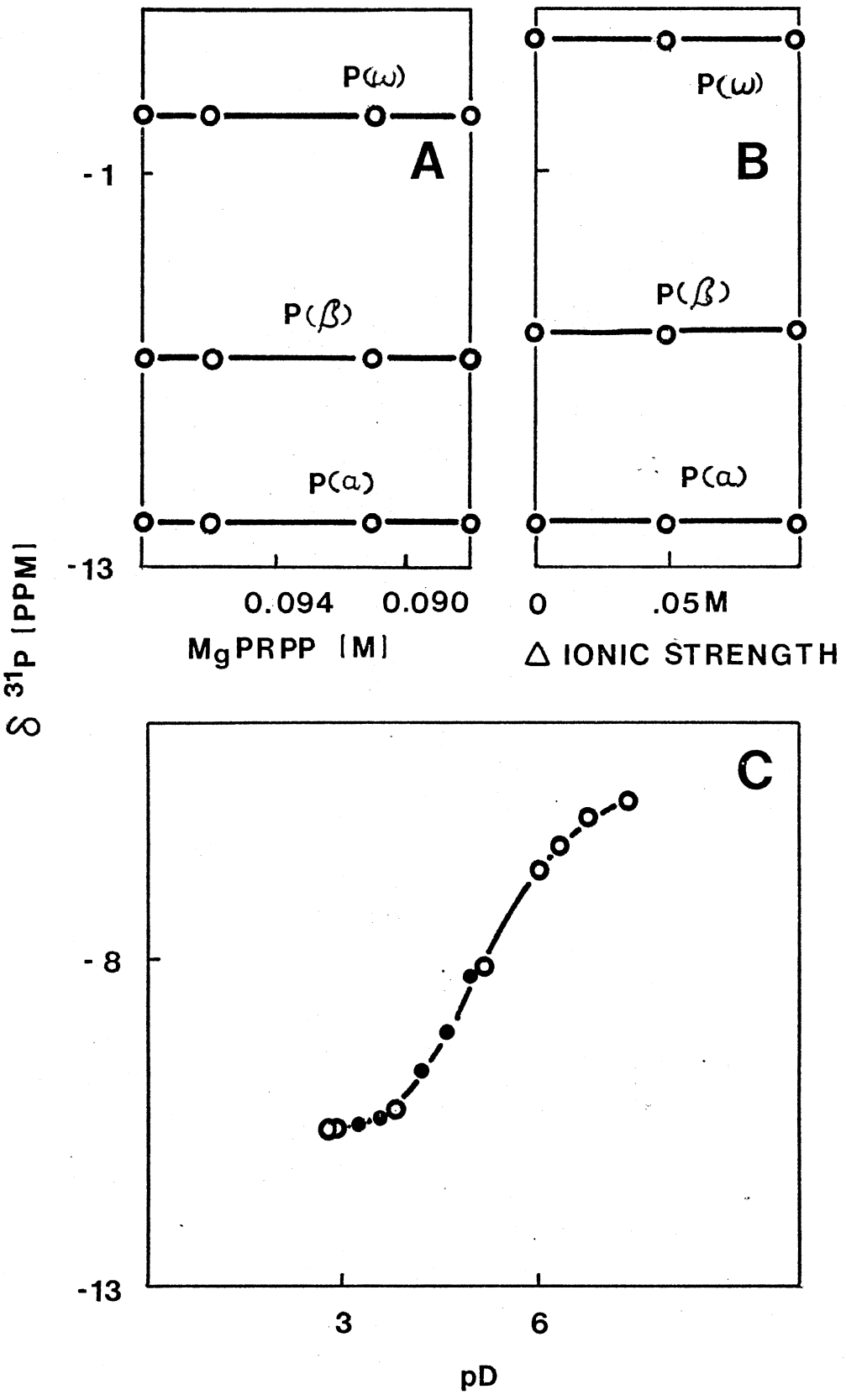
P(ω)
A
-1
P(β)
P(α)
-13
0.094
0.090
MgPRPP [M]
P(ω)
B
P(β)
P(α)
0
.05M
Δ IONIC STRENGTH
δ 31P [PPM]
C
-8
-13
3
6
pD

structure of MgPRPP, not Mg_2PRPP, equimolar Mg^{2+} was always used. Through use of the program COMICS (12) and inputing the apparent stability constants of H^+ and Mg^{2+} complexes of PRPP (6) we set an upper limit on the percent Mg^{2+} displaced by protons. At pH 3.5 22% of the PRPP molecules may exist as Mg^{2+}-free PRPP in the presence of equimolar Mg^{2+}. The presence of 25% excess Mg^{2+} lowers this estimate to 13%. The chemical shifts of the $^{31}\underline{P}(\beta)$ were measured versus pH in the presence of equimolar and 25% excess Mg^{2+}. This change in Mg^{2+} concentration and, therefore, change in amount of Mg^{2+}-free PRPP did not have a measureable effect on the chemical shift positions.

CHAPTER III

RESULTS AND DISCUSSION

Peak Assignments

^{31}P Peak Assignments

Figure 3 shows the ^{31}P spectra of PRPP. The spectra consists of three major signals: a triplet, a doublet, a quartet and some minor peaks. The minor signals are jedged to be impurities. As discussed under 'Materials", the PRPP in this sutdy contains approximately 15% phosphate containing impurities. The area of these minor peaks, 10%-15%, corresponds then to the amount expected on the basis of chemical analysis and the purity reported by Sigma. The major peaks have the same relative areas and their peak positions and splitting patterns correspond to that expected from the $^{31}\underline{P}(\omega)$, $^{31}\underline{P}(\beta)$, and $^{31}\underline{P}(\alpha)$ of PRPP as described next.

The triplet is assigned to the $^{31}\underline{P}(\omega)$ atom. Spin-spin coupling with the two equivalent protons, $\underline{H}(5)$, splits the $^{31}\underline{P}(\omega)$ signal into three peaks. Also, addition of ribose-5-phosphate (whose phosphorous is analogous to the $^{31}\underline{P}(\omega)$ atom of the PRPP) enriches the area of the triplet relative to the other two signals (Figure 4). Further evidence is that two other sugars with methylene bound monophosphates: 2,5-anhydro-D-glucitol 1,6-biphosphophosphate, and methyl β-D-fructofuranoside 1,6-biphosphate give rise to spectra containing triplets (13). The

Figure 3. ^{31}P NMR Spectra of 0.1 M PRPP in D_2O, pD = 9.00

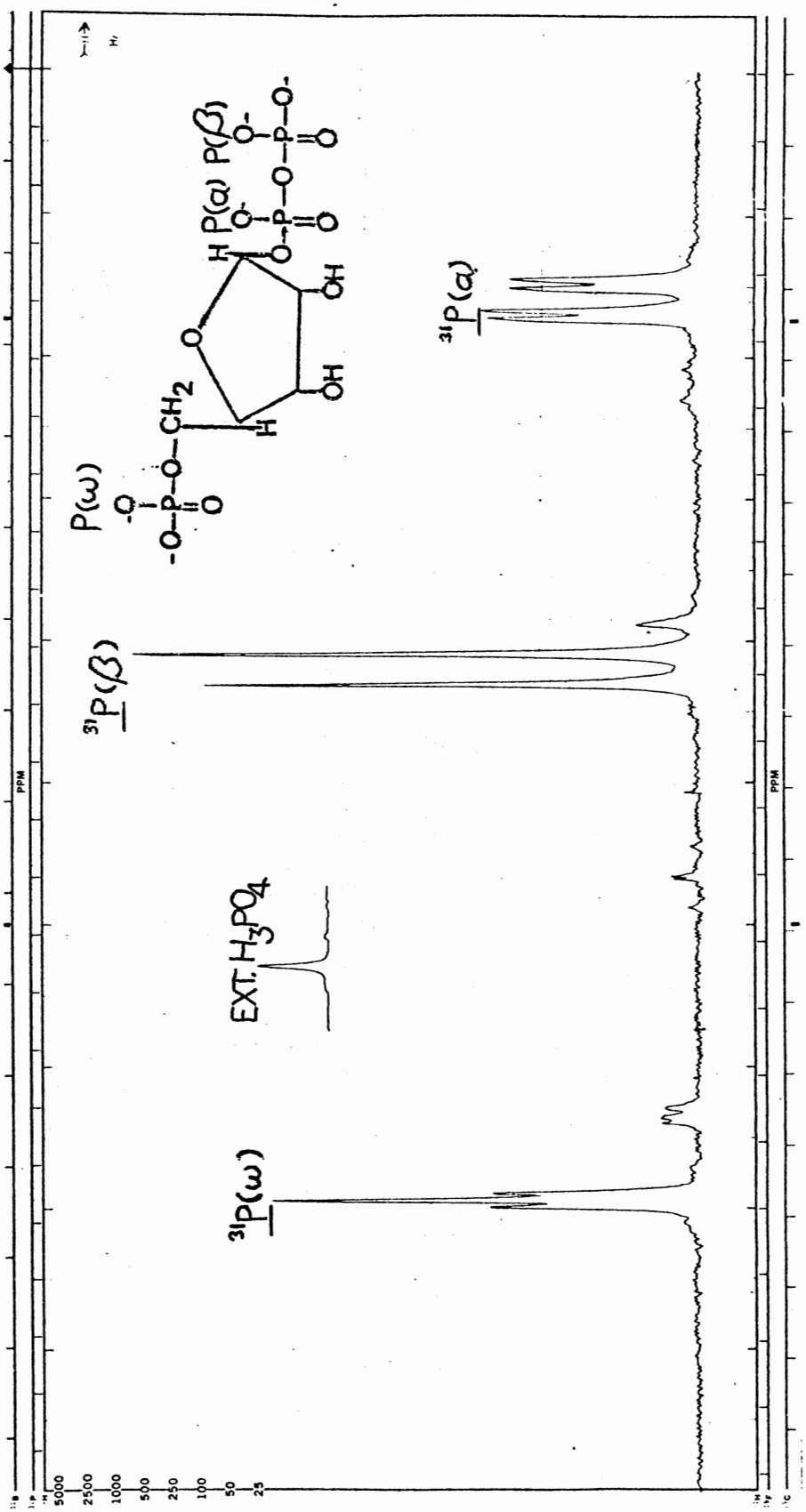
^{31}P(ω)
EXT. H_3PO_4
^{31}P(β)
P(ω)
P(α) P(β)
^{31}P(α)
PPM
PPM
5000
2500
1000
500
250
100
50
25

Figure 4. ^{31}P NMR Spectra of PRPP Plus Excess Ribose-5-Phosphate in D_2O

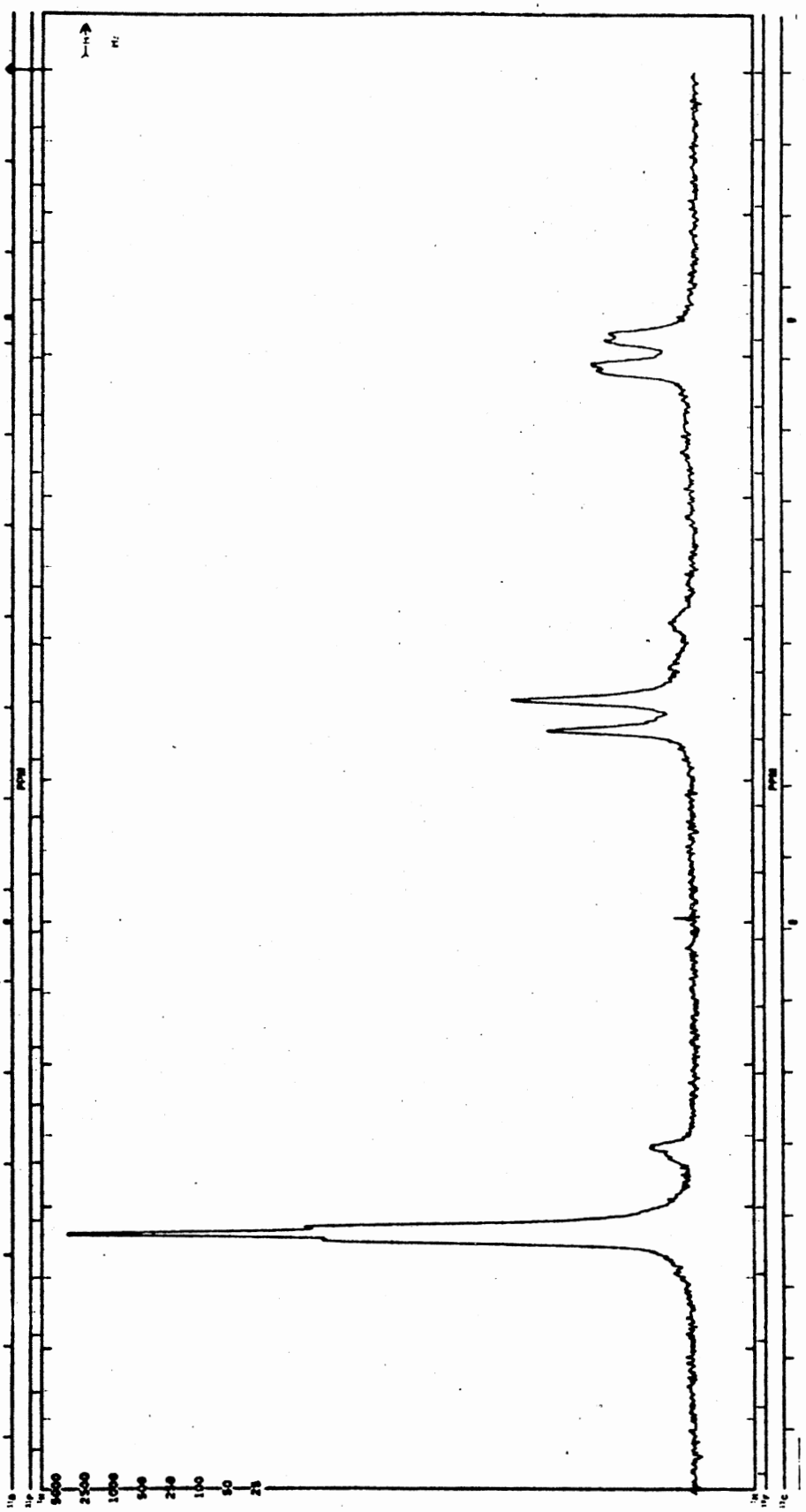

doublet is assigned to the $^{31}\underline{P}(\beta)$ atom. Its signal is split by the nonequivalent $^{31}\underline{P}(\alpha)$ atom. The equivalent phosphorous atoms in pyrophosphoric acid are in a similar environment as the $^{31}\underline{P}(\beta)$ atom in PRPP. When added in excess to a solution of PRPP, the ^{31}P signal from pyrophosphoric acid has nearly the same chemical shift as the doublet in the spectrum of uncontaminated PRPP (Figure 5). The quartet corresponds to the predicted splitting of the $^{31}\underline{P}(\alpha)$ atom. The $^{31}\underline{P}(\alpha)$ signal is coupled to the nonequivalent nuclei, namely $\underline{H}(1)$ and $^{31}\underline{P}(\alpha)$.

^{13}C Peak Assignments

The $^{13}\underline{C}$ signals were assigned by comparing ^{13}C PRPP resonances and $^{31}PO^{13}C$ couplings to those of model compounds (Table I). The $^{13}\underline{C}(3)$ signal of PRPP can be positively assigned as it is the only singlet and the only atom removed four bonds from a phosphorous atom. The $^{3}J_{^{31}POC^{13}C}$ couplings were greater than the $^{2}J_{^{31}PO^{13}C}$ couplings in the model compounds. Correspondingly, the coupling constants of the signals assigned to the $^{13}\underline{C}(4)$ and $^{13}\underline{C}(2)$ atoms of PRPP were greater than the coupling constants of the signals assigned to the $^{13}\underline{C}(5)$ and $^{13}\underline{C}(1)$ atoms. The magnitude of the $^{31}PO^{13}C$ couplings and chemical shift positions of the signals assigned to the $^{13}\underline{C}(1)$, $^{13}\underline{C}(2)$, $^{13}\underline{C}(4)$, and $^{13}\underline{C}(5)$ atoms agree with those of the model compounds.

Titration Curves of PRPP and MgPRPP

Figure 6 shows how the chemical shifts of the three phosphates vary upon removal of the last ionizable protons through increasing pH (or pD). At a pH of 3 the most acidic protons have been removed leaving the following structure:

Figure 5. ^{31}P NMR Spectra of PRPP Plus Excess Pyrophosphoric Acid in D_2O

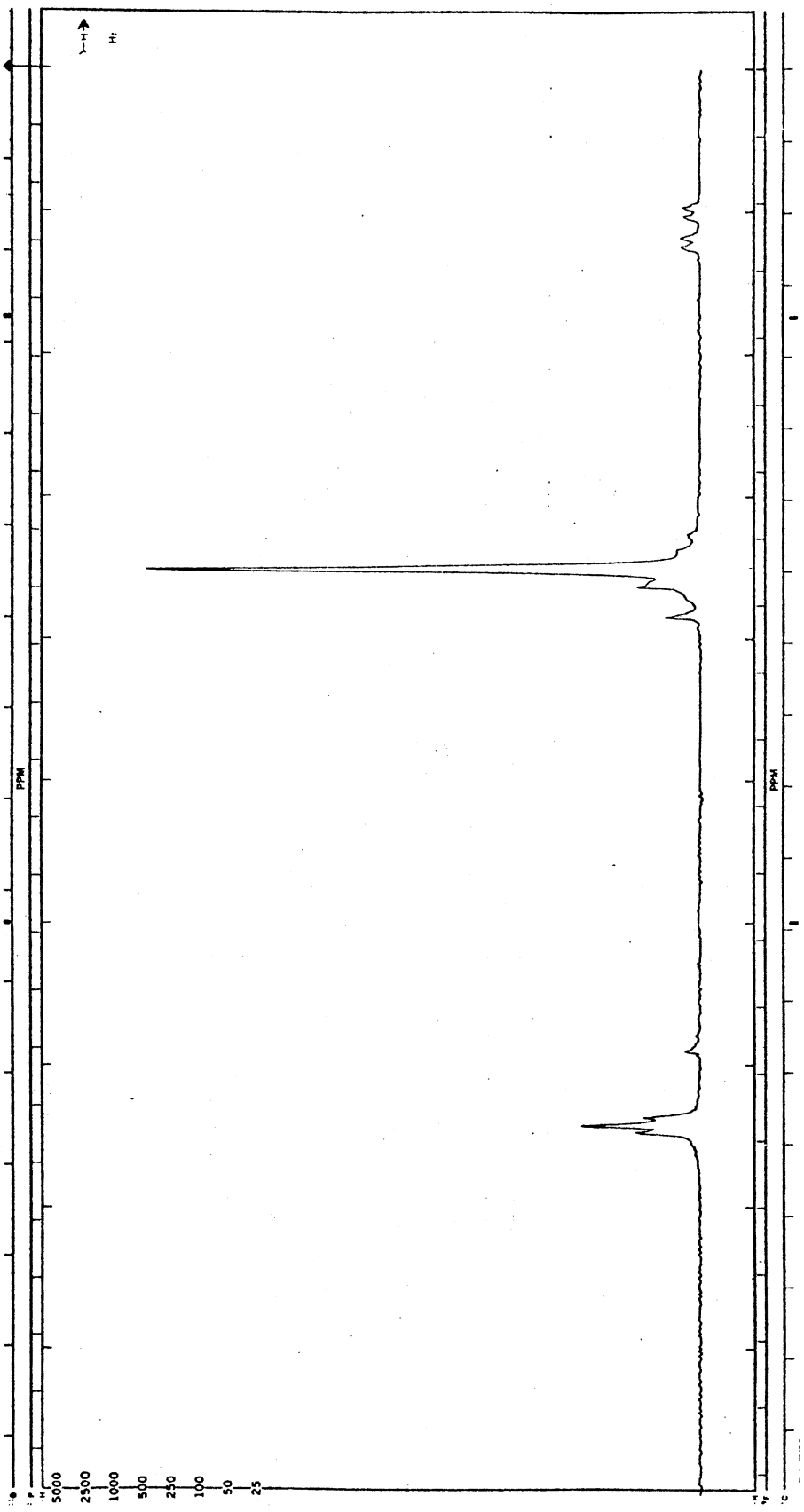
PPM
PPM
5000
2500
1000
500
250
100
50
25

TABLE I

^{13}C NMR DATA ON PRPP AND MODEL COMPOUNDS

Compound[a]	ppm (J_{pc} in Hz) from external TMS in D_2O				
	C(1)	C(2)	C(3)	C(4)	C(5)
PRPP	99.26 (5.72)	72.22 (6.14)	70.55	85.64 (8.19)	64.89 (4.33)
MgPRPP[b]	99.26 (5.31)	72.16 (7.29)	70.29	85.42 (7.98)	65.39 (2.82)
β-Ribose-5-Phosphate[c]	102.3	76.41	71.81	82.92 (8.71)	66.06 (4.51)
α-Ribose-5-Phosphate[c]	97.32	d	71.40	83.81 (9.52 Hz)	65.32 (broadened)
α-Fructose-6-Phosphate[e]	105.34	82.59	76.93	81.36 (8.1)	64.47 (2.8)
β-Fructose-6-Phosphate[e]	102.40	76.24	75.42	80.77 (7.3)	65.38 (4.2)
CMP[f]	89.4	70.0	74.6	83.6 (8)	63.6 (4)

[a] Numbering of carbons:

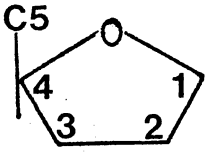

[b] Solution consisted of 0.2 M PRPP plus 0.2 M $MgCl_2$

[c] Assignments for ribose-5-phosphate were made by comparing the ^{13}C spectrum of a ribose-5-phosphate solution to the published spectrum (Birdsall, B., and Feeney, J. (1971) Chemical Communications, 1473-1474). 1474). The published data in dioxane was converted to the TMS scale using $\delta_c^{dioxane}$ = +67.40 ppm.

[d] Buried in ribose-5-phosphate β-3 resonance.

[e] Koerner, T. A. W., Cary, L. W., Bhacca, N. S., and Younathan, E. S. (1973) Biochemical and Biophysical Research Communications 51, 543-550.

[f] Converted from published data (Dorman, D. E., and Roberts, J. D. (1970) PNAS 65, 19-26) in CS_2 to the TMS scale ($\delta_c^{CS_2}$ - 192.8 ppm).

Figure 6. ^{31}P Chemical Shifts of PRPP Phosphorous atoms Versus pH. (——), signals from 0.1 M PRPP in 10% D_2O; (---), signals from 0.1 M PRPP plus 0.1 M $MgCl_2$ in 10% D_2O. Chemical shifts forming each pair of curves correspond to a separate phosphorous atom: $^{31}\underline{P}(\omega)$, $^{31}\underline{P}(\beta)$, and $^{31}\underline{P}(\alpha)$ from top to bottom.

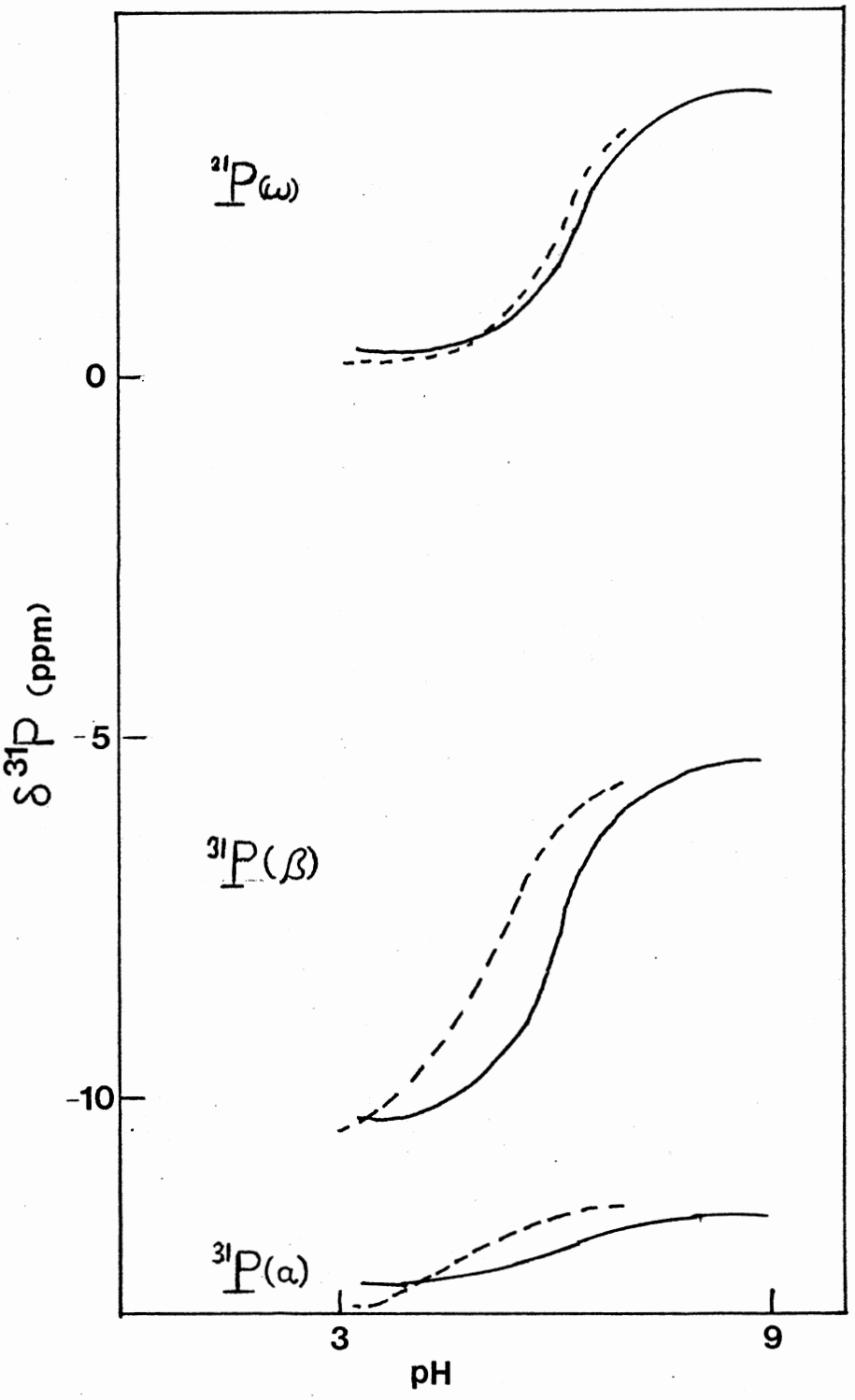
$^{31}P(\omega)$
0
$\delta^{31}P$ (ppm)
-5
$^{31}P(\beta)$
-10
$^{31}P(\alpha)$
3
9
pH

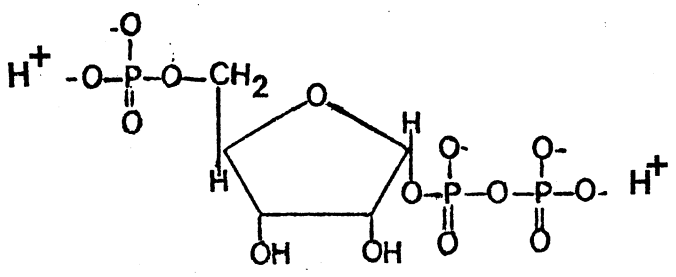

which has one dissociable proton on the pyrophosphate group and one on the monophosphate group. The ^{31}P chemical shifts of the phosphorous atoms in this state of protonation are approximately 0.4 ppm for the $^{31}\underline{P}(\omega)$, -10.5 ppm for the $^{31}\underline{P}(\beta)$, and -12.5 ppm for the $^{31}\underline{P}(\alpha)$. Removal of these last two ionizable protons causes the signal positions to shift to lower fields by approximately 4 ppm for the $^{31}\underline{P}(\omega)$, 5 ppm for the $^{31}\underline{P}(\beta)$, and 1 ppm for the $^{31}\underline{P}(\alpha)$. At pH values between the two equivalence points the solution contains a mixture of protonated and deprotonated C(5)-P and C(1)-PP. Instead of having a resonance for each structure, there is one signal position for each phosphate, which is the time average of the protonated and deprotonated signal positions. That is because the O-H bond allows rapid exchange of bound hydrogen with the solvent and the signal position of each phosphate becomes proportional to the average time the phosphate is protonated or deprotonated. This rapid exchange with H_2O also results in an absence of hydrogen phosphorous spin coupling (14).

Removal of only one proton from H_2PRPP^{3-} causes a shift in both the $^{31}\underline{P}(\alpha)$ and $^{31}\underline{P}(\beta)$ signals. It is reasonable that the proton is predominately bound to the P(β) since this P bears a doubly negative charge, and the proton binding causes a much greater perturbation of the $^{31}\underline{P}(\beta)$ signal than the $^{31}P(\alpha)$ signal. The inflection of the $^{31}\underline{P}(\alpha)$ has two possible explanations. It may be induced by the proton bound

to the P(β) through the H-O-P_β-O-P_α linkage. In contrast it may be caused by a sharing of proton binding between the P(α) and P(β) with the proton bound the majority of the time to P(β).

Mg^{2+} binding deshields the phosphates, shifting their signals to lower fields. Figure 6 shows that titration curves of all three phosphorous atoms shift to lower fields when PRPP is mixed with equimolar Mg^{2+}. (The effect was reproduced from a mixture of equimolar PRPP plus Mg^{2+} in D_2O.) This indicates that Mg^{2+} is interacting to some extent at all three sites.

pK_a's were estimated from the titration curves by finding the maxima of the slope replots ($\Delta \delta^{31}P/\Delta pH$ versus pH) (Table III). Data were obtained for D^+ binding as well as H^+ binding and both give the same qualitative results. In the absence of Mg^{2+} the P(ω) and P(β) have similar pK_a's. Mg^{2+} binding increases the acidity of the P(β), as shown by decrease of more than 1 pK_a unit at that site. Mg^{2+} binding does not change the P(ω) pK_a. This indicates little Mg^{2+} interaction at the P(ω) site compared to the P(β) site.

Changes in ^{31}P Chemical Shifts

Excess $MgCl_2$ was added to a PRPP solution causing formation of a mixture of MgPRPP and Mg_2PRPP (Figure 1). Up to a three-fold excess Mg^{2+} was added which was the solubility limit. Changes in the chemical shifts of $^{31}\underline{P}(\alpha)$ and $^{31}\underline{P}(\beta)$ appear to have reached a maximum upon the addition of equimolar Mg^{2+} whereas the $^{31}\underline{P}(\omega)$ signal continues to shift downfield with increasing Mg^{2+} concentration. These results were reproduced in a similar experiment using PRPP in D_2O rather than H_2O.

TABLE II

SUMMARY OF pK_a's[a]

Mg^{2+} (M)	Isotope	Phosphate	
		P(ω)	P(β)
0	H^+	6.25 ± .05	6.10 ± .1
0.1	H^+	6.28 ± .1	5.00 ± .005
0	D^+	6.7 ± .1	6.6 ± .15
0.1	D^+	6.7 ± .15	5.0 ± .15

[a]Titration curves of $\delta^{31}P$ versus pH (or pD) were obtained from 0.1 M PRPP in the presence and absence of 0.1 M $MgCl_2$, and in both 100% D_2O and 10% D_2O. pK_a's were obtained from the maxima of the slope replots, $\Delta\delta^{31}P/\Delta pH$ versus pH. Errors are the maximum deviations in locating the slope replot maxima.

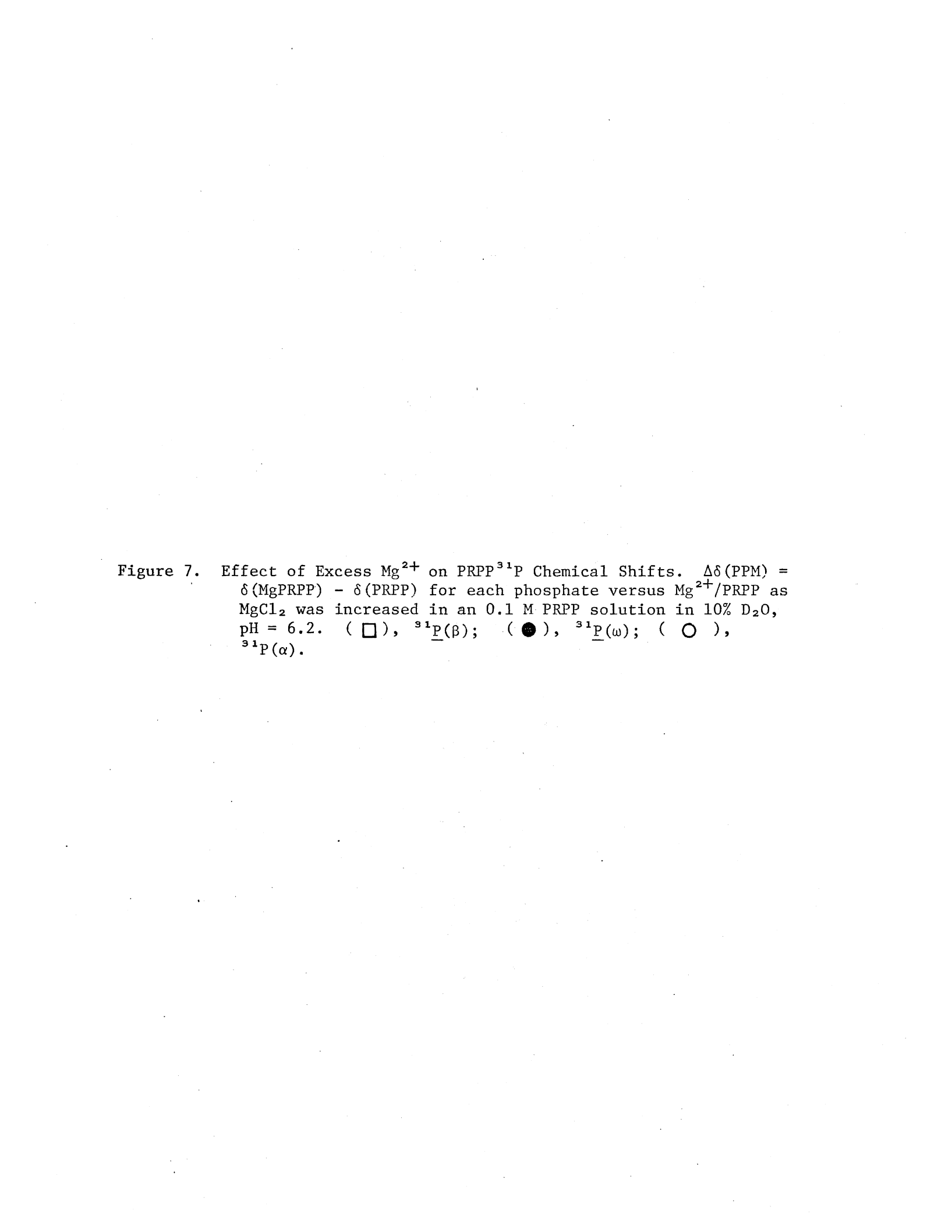

Figure 7. Effect of Excess Mg^{2+} on PRPP ^{31}P Chemical Shifts. $\Delta\delta$(PPM) = δ(MgPRPP) - δ(PRPP) for each phosphate versus Mg^{2+}/PRPP as $MgCl_2$ was increased in an 0.1 M PRPP solution in 10% D_2O, pH = 6.2. (□), $^{31}\underline{P}(\beta)$; (●), $^{31}\underline{P}(\omega)$; (○), $^{31}P(\alpha)$.

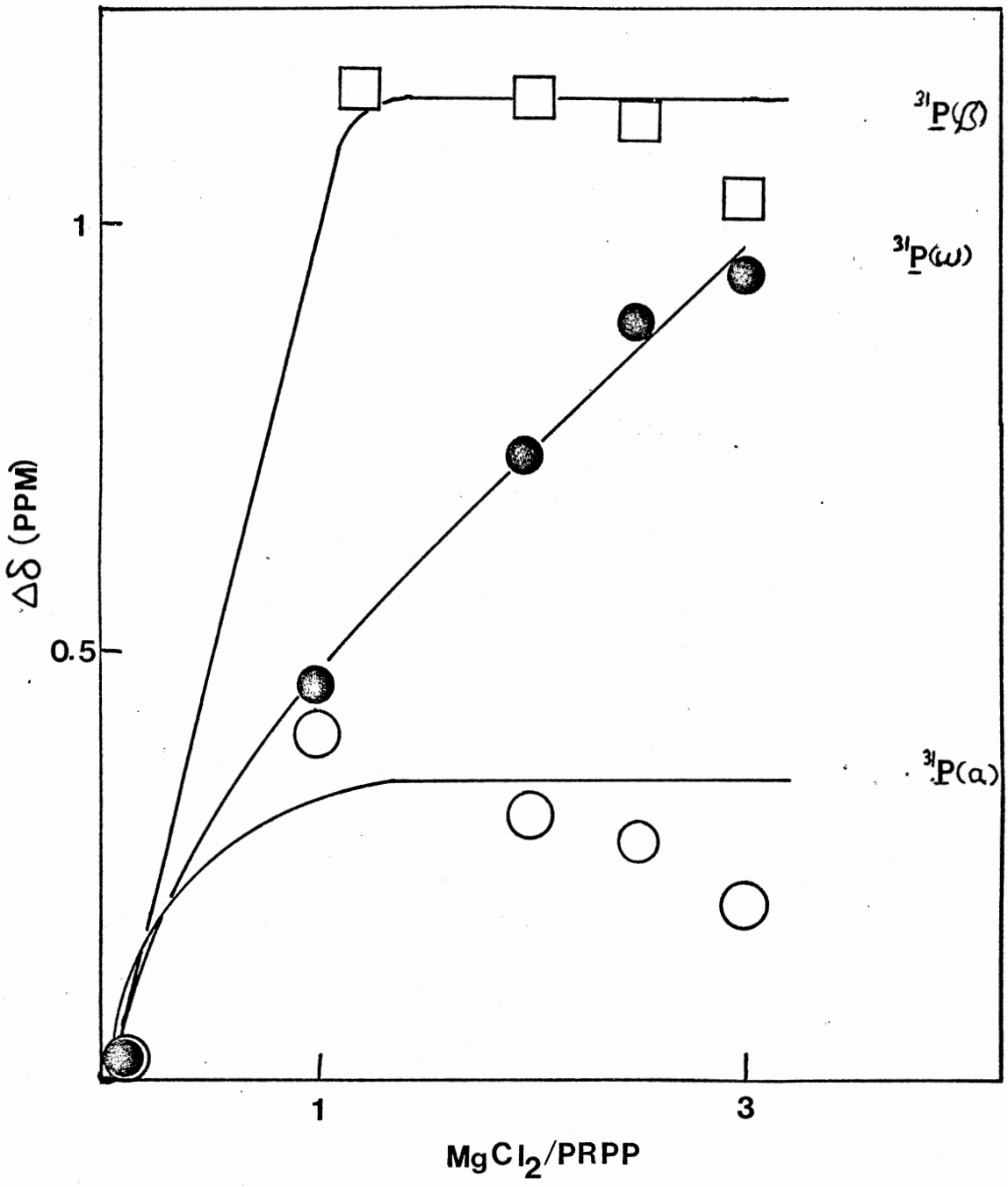
^{31}P(β)
^{31}P(ω)
^{31}P(α)
1
0.5
Δδ (PPM)
1
3
MgCl$_2$/PRPP

Spin-Spin Coupling Through the C(5)-O-P Bond

Equimolar Mg^{2+} binding to PRPP caused the POC(5) coupling to decrease from 4.33 Hz to 2.82 Hz while causing no significant change in the other POC couplings (Table I). This indicates the Mg^{2+} does interact with the P(ω).

TABLE III

SPIN-SPIN COUPLING IN THE PRESENCE AND ABSENCE OF Mg^{2+}

Spectra	Mg^{2+}	$J_{^{31}PO^{13}C_5}$	$J_{^{31}POC_5\ ^{1}H}$
^{13}C	+	8.19 (H_2)[a]	
^{13}C	-	7.98 (H_2)[b]	
^{31}P	+		5.08 (H_2)[c]
^{31}P	-		5.00 (H_2)[d]

[a] 0.2 M PRPP and 0.2 M $MgCl_2$ in D_2O

[b] 0.2 M PRPP in D_2O

[c] 0.1 M PRPP and 0.1 M $MgCl_2$ in 10% D_2O, pH = 5.2

[d] 0.1 M PRPP in D_2O, pD = 5.1

CHAPTER IV

SUMMARY AND CONCLUSIONS

The Courtauld space filling model demonstrated a variety of possible structures for MgPRPP (Figure 1). Two types of NMR data indicate that structure A is the major structure. 1) ^{31}P chemical shift changes indicate that stoichiometric concentrations of Mg^{2+} and PRPP nearly saturate Mg^{2+} binding at the C(1)-PP group, while the P(ω) is only partially complexed (Figure 7). 2) Mg^{2+} binding to a large fraction of the P(ω) should considerably increase the acidity of that group by neutralizing two negative charges. However, the pK_a (Table II) of the P(ω) of MgPRPP is unaffected. This is in contrast to the effect of stoichiometric Mg^{2+} on the C(1)-βP pK_a, which is decreased by more than 1 pK_a unit. Two types of data indicate that some fraction of the equimolar Mg^{2+} does interact with the P(ω): Mg^{2+} binding causes a small downfield shift of the $^{31}\underline{P}(\omega)$ signal (Figure 6) and decreases the $\underline{POC}(5)$ coupling by 1.51 Hz (Table I). This interaction is most reasonably explained on the basis of monodentate complexation of Mg^{2+} to the P(ω) even with only stoichemtric Mg^{2+} concentrations. In structures B through D of Figure 1, Mg^{2+} constrains the -C(5)P(ω) and -P(α)P(β) groups to part of a ring. This is in contrast to structure A which allows both groups to rotate freely in the presence and absence of Mg^{2+}. This would cause a major stereochemical change about the $\underline{POC}(5)$, $\underline{POC}(4)$, and $\underline{POC}(1)$, and $\underline{POC}(2)$ bonds

and likely change all four couplings. However, equimolar Mg^{2+} binding altered only the POC(5) coupling. This can be most simply explained by the fact that some fraction of the Mg^{2+} formed a monodentate complex with the P(ω) rather than any of structures B through D. One can then speculate that monodentate complexation has a greater affect on the stereochemistry about the POC(5) bond than bidentate complexation of the remaining Mg^{2+} (to the C(1) pyrophosphate) on the POC(1) stereochemistry. 2) Calculation (Appendix) on the basis of microscopic Mg^{2+} binding constants show that at least 7% of equimolar Mg^{2+} can exist in a monodentate complex with the P(ω).

In summary, though Courtauld modelling indicates that Mg^{2+} can theoretically form a bidentate complex with phosphates on both sides of the ring, NMR data indicate that bidentate complexation with the 1-pyrophosphate group is the main form of Mg^{2+} binding. On the basis of microscopic Mg^{2+} binding constants, the Mg^{2+} bound P(ω) probably exists as the monodentate complex. The equilibrium model scheme is shown in Figure 8.

Two questions had been raised by the previous study of Mg^{2+} and H^{+} binding to PRPP (6) as discussed in the Introduction. 1) Was the correct equilibrium model scheme assumed? That is a model in which Mg^{2+} binds to the C(1)-PP and also with lower affinity to the P(ω)? As shown in Figure 8, this study supports the validity of that model. 2) Why was the pK_a for Mg•H•PRPP of 4.2 (6) nearly one pK_a unit below the 5.1 value for MgADP (8)? ^{31}P NMR measurements of this study gave a pK_a of 5.0 (Table II) which is in agreement with pK_a value for MgADP determined by NMR also. The reason for the discrepancy between the NMR and pH titration methods is not understood at this time.

Figure 8. Equilibrium Model Scheme for Equimolar Mg^{2+} Binding to PRPP. Symbols to the right and left of L, PP and P, represent C(1)-PP and P(ω), respectively. M represents Mg^{2+}. The major structure is PLPP•M.

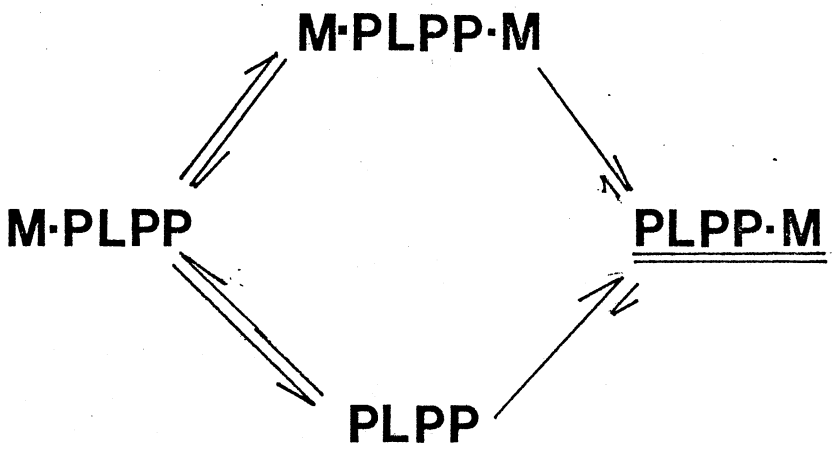
M·PLPP·M
M·PLPP
PLPP·M
PLPP

A SELECTED BIBLIOGRAPHY

(1) Lehninger, A. L. (1975) Biochemistry, Worth Publishers, New York.

(2) Mahler, H. R., and Cordes, E. H. (1971) Biological Chemistry, Harper and Row Publishers, New York.

(3) Krenitsky, T. A., Neil, S. M., Elion, G. B., and Hitchings, G. H. (1969) J. Biol. Chem., 244, 4779-4784.

(4) Switzer, R. L. (1971) J. Biol. Chem., 246, 2447-2458.

(5) Morrison, and Cleland (1966) J. Biol. Chem., 241, 673-683.

(6) Thompson, R. E., Li, E. L. F., Spivey, H. O., Chandler, J. P., Katz, A. J., and Appleman, J. R. (1978) Bioinorganic Chemistry, 9, 34-45.

(7) Rossotti, H. (1961) The Determination of Stability Constants, McGraw-Hill, New York.

(8) Phillips, R. C., Philip George, S. J., and Rutman, R. J. (1966) J. Amer. Chem. Soc., 88, 2631-2635.

(9) Nageswara RaO, B. D., and Cohn, M. (1977) J. Biol. Chem., 252, 3344-3350.

(10) Johnson, M. J. (1960) The Enzymes, Vol. 2, P. D. Boyer, H. Lardy, and K. Myrback, eds., Academic Press, New York, 415.

(11) Bates, R. G. (1973) Determination of pH; Theory and Practice, Wiley Publ., New York.

(12) Perrin, D. D., and Sayce, I. G. (1967) Talanta, 14, 833-842.

(13) Gray, G. R. (1976) Accounts of Chemical Research, 9, 418-424.

(14) Crutchfield, M. M., Callis, C. F., Irani, R. R. and Roth, G. C. (1962) Inorganic Chem., 1, 813-817.

APPENDIX

APPENDIX

WHAT % PRPP IS COMPLEXED BY Mg^{2+} AT THE C(5)-PHOSPHATE

Let symbols on right and left of L represent complexation to the C(1)-PP and C(5)-P, respectively. The model equilibrium scheme is

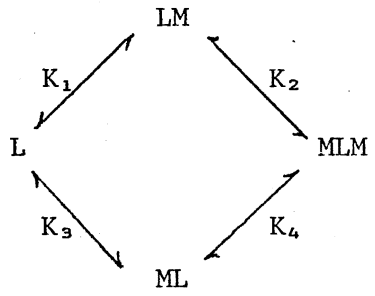

(1)

where L represents PRPP, M represents Mg^{2+} and $K_1 = 1.5 \times 10^3\ M^{-1}$, $K_2 = 46\ M^{-1}$, $K_3 = 58\ M^{-1}$, $K_4 = 1.20 \times 10^3\ M^{-1}$ from a previous study of Mg^{2+} binding to PRPP (8).[1] Then

$$TM = LM + ML + 2MLM + M \simeq LM + ML + 2MLM \quad (2)$$

$$TL = L + LM + ML + MLM \quad (3)$$

$$TM = [(K_1 + K_3)M + 2(K_1K_2M^2)]L + M \quad (4)$$

$$TL = [1 + (K_1 + K_3)M + K_1K_2M^2]L \quad (5)$$

$$L = TL/[1 + (K_1 + K_3)M + K_1K_2M^2] \quad (6)$$

[1] Since the C(1)-PP and C(5)-P association constants were consistent with those of ADP and AMP, respectively, we concluded that these phosphates bound Mg^{2+} independently of each other to a first approximation. A second order correction for the electrostatic effect of the two phosphates on each other was estimated and found to be insignificant.

$$TM = \frac{[(K_1 + K_3)M + 2K_1K_2M^2]TL}{1 + (K_1 + K_2)M + K_1K_2M^2} + M \tag{7}$$

In the experiments of this thesis

$$TL = 0.1\ M \tag{8}$$

$$TM = 0.1\ M \tag{9}$$

and

$$(K_1 + K_3) = 1558 \tag{10}$$

$$K_1K_2 = 6.9 \times 10^4 \tag{11}$$

Substituting 8-11 into 7 gives

$$0.1 = \frac{(1559\ M + 1.38 \times 10^5\ M^2)\ 0.1\ M}{1 + 1558\ M + 6.9 \times 10^4\ M^2} \tag{12}$$

Solving 12 numerically yields

$$M = 3.34 \times 10^{-3}\ M \tag{13}$$

Substituting 8, 10, 11 and 13 into 6 gives

$$L = 7.194 \times 10^{-3}\ M \tag{14}$$

Then

$$ML = K_3(M)(L) = 1.394 \times 10^{-3}\ M$$

$$MLM = K_1K_2(1)(M)^2 = 5.54 \times 10^{-3}\ M$$

$$\frac{ML + MLM}{TL} = 6.93 \times 10^{-2}$$

Therefore, the percent of 0.1 M PRPP which has Mg^{2+} (0.1 M) bound to the C(5)-P equals approximately 7%.

VITA

Teresa Ann Webster

Candidate for the Degree of

Doctor of Philosophy

Thesis: I. POLYMER INDUCED ASSOCIATION AND KINETICS OF OXALOACETATE UTILIZING ENZYMES
II. PROTON AND MAGNESIUM BINDING TO 5-PHOSPHORIBOSYL α-1-PYROPHOSPHATE

Major Field: Biochemistry

Biographical:

Personal Data: Born in Spokane, Washington, July 19, 1953, the daughter of Lawrence A. and Eleanor Hoerner.

Educational: Graduated from Shadle Park High School, Spokane, Washington, in 1971; received the Bachelor of Science degree in Chemistry from Eastern Washington State University, Cheney, Washington, in 1976; completed requirements for the Doctor of Philosophy degree at Oklahoma State University on December, 1980.

Professional Experience: Undergraduate teaching assistant from June 1974 to August 1975, Department of Chemistry, Eastern Washington State University; Research Assistant, from August 1976 to August 1980, Oklahoma State University Biochemistry Department.

Honorary Societies: Sigma Xi, Phi Lambda Upsilon.